Band Structure of Transition Metals and Their Alloys

JOHN B. GOODENOUGH
Lincoln Laboratory, Massachusetts Institute of Technology, Lexington, Massachusetts*
(Received September 15, 1958; revised manuscript received May 20, 1960)

A departure from the conventional approach to the energy-band problem is achieved in three ways. First, it is noted that there is a critical atomic separation $R_c \lesssim (2.9 \pm 0.1)$ A such that for $R < R_c$ electrons from atomic 3*d* orbitals that are directed along a ligand must be treated as collective electrons, for $R > R_c$ the corresponding electrons are localized, Heitler-London electrons. Since the 3*d* wave functions are anisotropic, this implies that there may be localized and collective 3*d* electrons simultaneously present. Second, it is pointed out that localized electrons obey Hund's rule and may therefore contribute an atomic moment. This means the corresponding energy levels, or narrow bands, are split into discrete subbands. Any moment from collective 3*d* electrons is induced by the simultaneously present localized electrons via intra-atomic exchange. Third, it is asserted that if nearest-neighbor antiferromagnetic order can be propagated throughout a lattice and the nearest-neighbor-directed 3*d* orbitals are half-or-less filled, the collective electrons ($R < R_c$) can be stabilized by bonding-band formation. If the orbitals are more than half filled, the "extra" electrons cannot be stabilized by antiferromagnetic correlations between nearest neighbors. If antiferromagnetic, nearest-neighbor order is not possible, the electrons form a conventional metallic band. These observations provide sharp criteria for Pauli paramagnetism, antiferromagnetism, ferrimagnetism, and ferromagnetism in transition metals and their alloys. They are used to explicitly introduce electron correlations into the construction of qualitative energy diagrams from which semiempirical density-of-states curves are constructed. The resulting model is shown to provide a consistent interpretation of phase stability, magnetic properties, electronic specific heats, Hall effect data, and form-factor measurements for the bcc and close-packed transition metals of the first long period and their alloys. The model is only partially successful for elements of the second and third long periods.

I. STATEMENT OF POSTULATES

QUANTITATIVE calculations of the band structure of metals are plagued by the mathematical difficulties associated with an adequate treatment of the electron-correlation problem.[1] The purpose of the present paper is to suggest three postulates that are related to the electron-correlation problem and appear to be important for the transition metals and their alloys.

Postulate I. Localized (Heitler-London "quasi" particles) and collective 3d *electrons may be simultaneously present at a transition element in a solid.*

This assertion is based on the fact that the 3*d* wave functions are anisotropic. The successful description by ligand-field theory of both magnetic and crystallographic properties of transition-element cations in ionic insulators and semiconductors has emphasized the importance of the relative symmetries of the 3*d* wave functions and the nearest-neighbor configuration. The fivefold degeneracy of atomic 3*d* wave functions is removed by simple symmetry considerations, and this fact implies that crystalline states formed from 3*d* wave functions may be separable into 3*d* subbands such that there is little admixing of states with differing symmetry relative to the lattice. A subband is here defined as a set of states with contiguous energies that have been formed from linear combinations of atomic orbitals of analogous symmetry. The suggestion that some of the *d* electrons are localized, others are not, has been proposed in one form or another by several previous workers.[2–8] A comparison of these previous discussions with that proposed here can be found elsewhere.[9]

Theoretical arguments for a critical atom-atom separation R_c such that for $R > R_c$ the outer electrons are best described by a Heitler-London model, for $R < R_c$ by a collective-electron model, were first proposed by Mott.[10] Recent quantitative calculations for the N_2 molecule by Nesbet[11] have demonstrated that whereas there is covalent bonding of both the σ and π orbitals at the equilibrium separation, at twice the equilibrium separation it is necessary to start with Wannier, or localized wave functions if a good approximation of the energy is to be achieved by a single determinantal configuration: In fact, it was necessary to consider 64 configuration interactions to obtain equivalent energies from molecular orbitals. At intermediate separations, the best initial one-electron functions were found to be Wannier functions for the π electrons, molecular functions for the σ electrons. It should be noted that these results imply that any quantitative calculation for the band structure of the transition metals that uses a single Slater determinant in which all 3*d* electrons are treated similarly must be considered suspect if sym-

* Operated with support from the U. S. Army, Navy, and Air Force.

[1] P. Löwdin, in *Advances in Chemical Physics*, edited by I. Prigogine (Interscience Publishers, Inc., New York, 1959), Vol. II, pp. 207–322.

[2] L. Pauling, Phys. Rev. **54**, 899 (1938).
[3] F. Bader, K. Ganzhorn, and U. Dehlinger, Z. Physik **137**, 190 (1954).
[4] J. S. Griffith, J. Inorg. Nuclear Chem. **3**, 15 (1956).
[5] N. F. Mott and K. W. H. Stevens, Phil. Mag. **2**, 1364 (1957).
[6] J. S. Griffith and L. E. Orgel, Nature **181**, 170 (1958).
[7] J. B. Goodenough, J. Appl. Phys. **29**, 513 (1958).
[8] W. M. Lomer and W. Marshall, Phil. Mag. **3**, 185 (1958).
[9] J. B. Goodenough, Lincoln Laboratory Technical Report TR-208, September 1, 1959 (unpublished).
[10] N. F. Mott, Proc. Phys. Soc. (London) **A62**, 416 (1949).
[11] R. K. Nesbet, Neutron Diffraction Conference, Gatlinburg, Tennessee, April, 1960 (unpublished).

metry considerations suggest that some of the 3*d* electrons are localized. Coulson and Fischer[12] have also demonstrated how the single-determinant solution rapidly breaks down for the H_2 molecule at interatomic distances somewhat larger than the equilibrium distance.

Experimentally, consideration[13] of the electric, crystallographic, and magnetic properties of the corundum-type sesquioxides and of the rocksalt-type nitrides and oxides of Ti, V, Cr, and Fe suggests that *the critical separation for cations with 3d outer electrons is* $R_c \lesssim (2.9 \pm 0.1)$ A. Although relative ion size may indeed contribute to the particular phase transformation encountered in several of these compounds, there is strong evidence for metal-metal bonding via the 3*d* electrons in the low-temperature phases. Further, Ti_2O_3 and V_2O_3 are ionic and simultaneously metallic at high temperatures. There are two metal-metal distances in the corundum structure, and $Ti^{3+}(3d^1)$, $V^{3+}(3d^2)$ have one and two phase transformations, respectively, as a result of metal-metal bonding.[13] This indicates that the two 3*d* electrons of V^{3+} act independently of one another, or that symmetry may cause even the collective electrons to occupy discrete subbands.

Postulate II. In metals, localized 3d *electrons obey Hund's rule and may therefore introduce a localized atomic moment.*

Localized 3*d* electrons are commonly found in ionic compounds containing transition-element cations. These electrons are found to obey Hund's rule except in those cases where the ligand fields are stronger than the intra-atomic exchange fields. Since this condition only exists if the ions have relatively high charge, it is reasonable to assume that in metals the intra-atomic exchange fields are the stronger.

Postulate III. Superexchange ($R > R_c$) *or bonding-band* ($R < R_c$) *stabilization of the subband associated with nearest-neighbor-overlapping* 3d *orbitals can occur if it is possible to propagate antiferromagnetic nearest-neighbor order throughout the lattice and the overlapping orbitals are half-or-less filled. Nearest-neighbor interactions are stronger than next-nearest-neighbor interactions.*

(If there is no 3*d* subband associated with nearest neighbors, substitute "next-nearest" for "nearest.")

Superexchange stabilization has been discussed by Anderson[14] and Nesbet.[15] Although these ideas have been principally applied to oxides in which the superexchange mechanism occurs via an intervening O^{2-} ion, it is obvious that if there is direct overlap of localized orbitals that are half-or-less filled, a stabilization due to admixture of excited states corresponding to the transfer of an electron from one atom to its nearest neighbors can occur provided it is possible to propagate antiferromagnetic nearest-neighbor order. With relatively small overlap of localized orbitals, the probability of electron transfer is small so that the electrons remain essentially localized; however, the superexchange stabilization introduces antiferromagnetic coupling and an incipient covalency. With relatively large orbital overlap, there is a large probability of electron transfer so that the electrons at any atom are essentially spin-paired; this situation corresponds to that found in a diamagnetic covalent bond.

In the conventional covalent-bond model, there are two electrons associated with a given ligand. Thus, in the diamond structures of C, Si, Ge, and Sn each atom has four nearest neighbors, and the valence band is filled with four electrons per atom. However, chemists have noted that this concept must be generalized, and such nomenclature as "resonating bonds," "pivotal resonance," and "half bonds" has been introduced. The essential requirements in each case are (1) the ability to propagate antiferromagnetic nearest-neighbor order, and (2) outer-electron orbitals, permitted nearest-neighbor overlap by symmetry considerations, that are half filled. If there are two atoms per unit cell, the band formed from the overlapping orbitals may be split in two. As in the case of diamond-type structures, this gives rise to a filled subband (bonding band or valence band) with only one electron per band-participating atomic orbital.

If antiferromagnetic nearest-neighbor order can be propagated (two atomic sublattices), but the nearest-neighbor-overlapping orbitals are more than half filled, then the superexchange mechanism is inhibited since the available nearest-neighbor orbitals are all partially occupied. However, an alternate exchange mechanism can be formulated. Imagine a band that is three fourths filled. If all of the orbitals corresponding to spin α are filled, then stabilization can occur via resonance of the spin β electrons between the two atomic sublattices. *This mechanism introduces a net ferromagnetism equivalent to a magnetization of those electrons in excess of a half-filled band.*

Experimental support for these concepts is found in the magnetic properties of the diatomic molecules. The only two common, paramagnetic gases are O_2 and NO. Other important diatomic molecules have $^1\Sigma$ normal states and are diamagnetic. The nitrogen atom has the outer-electron configuration s^2p^3, and therefore all three p electrons are available for covalent bonding in the N_2 molecule: one p_σ and two p_π bonds. Therefore the N_2 molecule is diamagnetic and extremely stable. The oxygen atom (s^2p^4) has one extra p electron. Therefore, in NO there is one extra p_π electron and in O_2 there are two extra p_π electrons. In support of the above arguments, the ground states of NO and O_2 are, respectively, $^2\Pi$ and $^3\Sigma$. The diatomic halogen molecules are again diamagnetic since the p_π orbitals are full and the p_σ orbitals are still only half filled.

There remains the lattice type in which it is not possible to propagate antiferromagnetic nearest-

[12] C. A. Coulson and I. Fischer, Phil. Mag. **40**, 386 (1948).
[13] J. B. Goodenough, Phys. Rev. **117**, 1442 (1960).
[14] P. W. Anderson, Phys. Rev. **115**, 2 (1959).
[15] R. K. Nesbet, (to be published).

TABLE I. Relation between d-orbital vs neighbor-configuration symmetry, band occupation and band characteristics in pure metals. n.n.=near-neighbor; n.n.n.=next-near-neighbor; μ_s=contribution to spontaneous atomic moment; μ_B=Bohr magneton; n and n_h are, respectively, the number of electrons or holes per atom in a n.n.n.-directed orbital, m_h for a n.n.-directed orbital; ν is number of electrons in a half-filled, n.n.-directed band. Bonding conditions for n.n.n.-directed orbitals include sufficient orbital overlap for the formation of a n.n.n.-directed collective-electron band, or a n.n.n. separation that is smaller than some critical length that is characteristic of the atoms in question.

<table>
<tr><th>BANDS FROM n.n.n.-DIRECTED ORBITALS / BANDS FROM n.n.-DIRECTED ORBITALS</th><th>EMPTY</th><th>$\leq \frac{1}{2}$ FILLED AND BONDING CONDITIONS MET</th><th>BONDING CONDITIONS NOT MET</th><th>$> \frac{1}{2}$ FILLED AND BONDING CONDITIONS MET</th></tr>
<tr><td>EMPTY</td><td>—
—</td><td>BONDING: $\mu_S = 0\mu_B$
—</td><td>LOCALIZED: (↑↑) OR PARAMAG.
$\mu_S = n\mu_B$
—</td><td rowspan="2"></td></tr>
<tr><td>$\leq \frac{1}{2}$ FILLED AND BONDING CONDITIONS MET (ANTIFERROMAGNETIC)</td><td>—
BONDING: $\mu_S = 0\mu_B$</td><td colspan="2">LOCALIZED: (↑↑) WITHIN SUBLATTICE; (↑↓) BETWEEN SUBLATTICES
SUBLATTICE $\mu_S = n\mu_B$
BONDING: (↑↓) INDUCED $\mu_S \propto n\mu_B$</td></tr>
<tr><td>BONDING CONDITIONS NOT MET (FERROMAGNETIC)</td><td>—<br colspan="2">METALLIC: $\mu_S = 0\mu_B$</td><td>BONDING: $\mu_S = 0\mu_B$
LOCALIZED: (↑↑)
$\mu_S = n_h\mu_B$
(↑↓): $\mu_S = m_h\mu_B$</td><td></td></tr>
<tr><td>$> \frac{1}{2}$ FILLED AND BONDING CONDITIONS MET (FERROMAGNETIC)</td><td>—
$\mu_S = 0\mu_B$</td><td colspan="3">LOCALIZED: (↑↑)
$\mu_S = n\mu_B$ IF BAND $\leq \frac{1}{2}$ FILLED; $\mu_S = n_h\mu_B$ IF BAND $> \frac{1}{2}$ FILLED
(↑↓): $\mu_S = (m-\nu)\mu_B$ IF BAND $< \frac{3}{4}$ FILLED; $\mu_S = m_h\mu_B$ IF BAND $> \frac{3}{4}$ FILLED</td></tr>
</table>

neighbor order. In this case superexchange or bonding-band stabilization is not possible, and the collective electrons form a conventional "metallic" band in which the predominant electron correlation is probably that between electrons of parallel spins as introduced by the Pauli exclusion principle, or by antisymmetrized wave functions. It follows that $E_b(metallic) > E_b(valence)$, *and a narrow metallic band may be spontaneously magnetized if an atomic moment from localized electrons is simultaneously present.* The latter condition takes cognizance of the fact that any magnetization of a collective-electron band is at the expense of a broadening of the occupied portion of that band. E_t and E_b are the upper and lower bound of an energy band or subband.

Of particular interest for the theory of magnetism is not only the magnitude of the localized atomic moment, but also the sign of the magnetic coupling between neighboring atomic moments. These items are implicit in the previous discussion. Localized electrons in half-or-less filled orbitals split by Hund's rule are superexchange stabilized by antiferromagnetic coupling of the neighboring (next-nearest) atoms with which they directly interact (Postulate III). However, the atomic moments of nearest neighbors are coupled indirectly via the collective electrons. If the collective electrons are 3d electrons, then intra-atomic and nearest-neighbor exchange forces can be expected to be stronger than next-nearest-neighbor interactions (Postulate III). It follows from the above discussions that (1) Pauli paramagnetism exists if there are no atomic moments present from localized electrons, (2) antiferromagnetism exists at temperatures below a T_N if antiferromagnetic nearest-neighbor order can be propagated throughout the structure, localized atomic moments are present, and the nearest-neighbor-overlapping orbitals are half-or-less filled,[16] (3) ferromagnetism exists at temperatures below a T_C if localized atomic moments are present and nearest-neighbor-overlapping orbitals are either more than half-filled or metallic. Thus, it has been possible to make a sharp prediction about the conditions for Pauli paramagnetism, antiferromagnetism, and ferromagnetism. The arguments assume Russell Saunders coupling and therefore may not be appropriate for the heavier elements. These features are summarized in Table I. The bonding conditions referred to in Table I are the ability to propagate antiferromagnetic nearest-neighbor order and large overlap of nearest-neighbor orbitals. In the nomenclature to follow, a half-or-less filled band meeting

[16] In ordered alloys, nearest neighbors may not have available 3d states for band formation. In this case the relevant nearest neighbors may be next-nearest neighbors. See, for example, the discussion on ordered FeAl.

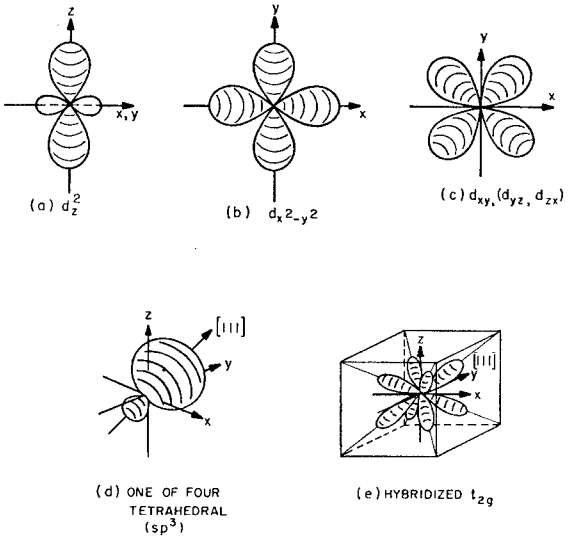

FIG. 1. Angular dependence for various atomic orbitals.

the bonding conditions is said to contain "bonding" electrons; the top half of such a band is said to contain "antibonding" states.

In closing this section, it seems worthwhile to emphasize that quantitative calculations that do not properly account for the spin-correlation stabilization discussed here are probably misleading. It is obvious that this effect is the source of the extreme stability of the N_2 molecule.

II. APPLICATION TO SPECIFIC STRUCTURES

A. Symmetry Considerations

Let the wave-function symmetry be always referred to a set of Cartesian coordinates centered at the atom in question. Figure 1 (a)-(e) shows the orientation of this coordinate system relative to the electron-density distributions of the five d states, the hybridized (sp^3) states, and the t_{2g} states (hybridized d_{xy}, d_{yz}, d_{zx} states). It is immediately seen that if the d-level degeneracy is removed by a splitting that leaves a doubly degenerate e_g level and a triply degenerate t_{2g} level, the electron-density distributions for the e_g and t_{2g} electrons, respectively, are directed along the ⟨100⟩ and ⟨111⟩ (or ⟨110⟩) axes of the Cartesian reference frame. Since the crystalline orbitals can be expected to retain the same angular symmetry as the atomic orbitals from which they are formed, symmetry considerations are referred to the easily visualized atomic orbitals. Further, the d orbitals are discussed separately from the s-p orbitals even though there must be admixing of orbitals belonging to the same representation. However, this simplification does not significantly influence the qualitative arguments developed below.

B. Body-Centered-Cubic Structure

Figure 2(a) shows the most reasonable configuration for the Cartesian reference frame relative to the bcc structure. Since it is possible to propagate antiferromagnetic nearest-neighbor order and nearest neighbors all lie along ⟨111⟩ axes of the reference frame, the magnetic character of the material is determined by whether the t_{2g} orbitals are half-or-less filled ($n_{2g} \leqslant 3$) or are more than half filled ($n_{2g} > 3$) and by the relative energies of the next-nearest-neighbor-directed e_g electrons.

1. Case $n_{2g} \leqslant 3$

Since the bonding conditions are met for the t_{2g} electrons [R(n.n.) $< R_c$], the bottom half of the t_{2g} band is stabilized. Therefore, the t_{2g} band has a bonding and antibonding half, and these two halves may be split in two if antiferromagnetically coupled atomic moments are simultaneously present.[17] Any inherent spin correlation between nearest neighbors, whether it be antiferromagnetic ($n_{2g} \leqslant 3$) or ferromagnetic ($n_{2g} > 3$), forces the next-nearest-neighbor correlations to be ferromagnetic. Therefore, the e_g electrons are forced to occupy antibonding states [R(n.n.n.) $\approx R_c$ in Cr, Fe]. As a result, the e_g electrons are localized and contribute an atomic moment.[18] The e_g band is therefore split into two subbands similar to localized orbitals split by intra-atomic exchange (Hund's rule). Since next-nearest-neighbor antibonding states are less stable than bonding states, but probably more stable than the nearest-neighbor antibonding states, the narrow, more stable e_g subband should lie at the top of the bonding half of the t_{2g} band as shown in Fig. 2(b). It should be noted that this energy diagram differs from that presented by Slater and Koster[19] in one important respect: Whereas the Slater-Koster density-of-states curve is symmetric about the d-band energy gap, the explicit spin-correlation considerations of this paper require a shifting of the lower e_g subband from the center to the top of the t_{2g} lower half-band; this represents a shift of $\sim$0.3 ev. It follows that if $n_{2g} \leqslant 3$, the bcc metal is Pauli paramagnetic if there are no e_g electrons present, is antiferromagnetic if e_g electrons are present.

2. Case $n_{2g} > 3$.

If $n_{2g} > 3$ and the e_g orbitals are half-or-less filled ($n_g \leqslant 2$) then the "extra" t_{2g} electrons ($n = n_{2g} - 3$) are spontaneously magnetized and couple nearest-neighbor e_g electrons ferromagnetically (see Table I). Further, an additional stabilization of the ferromagnetic electrons can be realized by the following electron correlation: When the ferromagnetic electrons (those responsible for the net atomic moment) are concentrated in e_g orbitals

[17] J. C. Slater, Phys. Rev. **82**, 538 (1951).

[18] Since the orbital momentum of the e_g electrons is quenched, this is approximately a spin-only atomic moment.

[19] J. C. Slater and G. F. Koster, Phys. Rev. **94**, 1498 (1954).

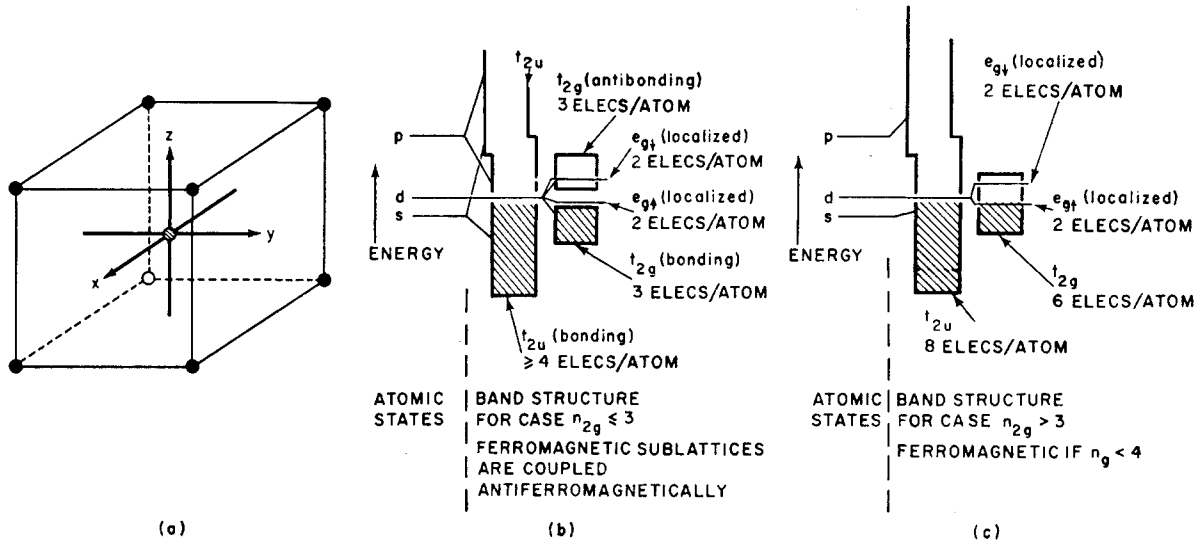

FIG. 2. Qualitative features of band structure for bcc transition metals.

on one atom, let all the ferromagnetic electrons of next-nearest neighbors be concentrated in t_{2g} orbitals. Such a correlation is only possible if there is ferromagnetism (some levels in top half of t_{2g} band occupied). Further, this correlation is an optimum if there are two ferromagnetic electrons per atom, corresponding to a half-filled e_g orbital. On the average, the ferromagnetic electrons occupy e_g and t_{2g} orbitals equally in this optimum configuration. Further the orbital momentum of the t_{2g} electrons is not quenched so that the ferromagnetic bcc metals can have a Landé g factor differing from the spin-only value of $g=2$. If this reasoning is correct, then α Fe can be expected to represent the optimum configuration, the extra $0.22\mu_B$ per atom coming from a combination of $g>2$ and a limited, induced magnetization of the $s-p$ electrons. The measured g factor for iron[20,21] is $g=2.12-2.14$. This case is illustrated schematically in Fig. 2(c).

3. *Stabilization of p electrons.*

In order that α Fe represent the optimum ferromagnetic configuration, it is necessary that there be three $s-p$ electrons ($n_{2u}=3$) since iron has a total of 8 outer electrons. Some quantitative calculations have assumed 0.22 $s-p$ electrons, others estimate about one $s-p$ electron. Thus there appears to be an essential conflict between the model proposed here and the estimates of previous workers. On theoretical grounds, the symmetry of the bcc structure is ideal for strong bonding-band stabilization of the $s-p$ electrons since the (sp^3) orbitals are directed along the ⟨111⟩ axes towards nearest neighbors. It is proposed here that this stabilization causes the formation of an $s-p$ bonding band that overlaps considerably the narrower d bands. This band is labelled t_{2u} in Fig. 2. For further suport of the case for $n_{2u}\approx 3$, consider the following experimental facts.

(a) The bcc metals Ti, Zr; V, Nb, Ta; Cr, Mo, W; Mn are all Pauli paramagnetic or (Cr,δMn) antiferromagnetic. This is consistent with the model if $n_{2u}=3$.

(b) Soft x-ray K emission does occur in V, Cr, and Fe even though transitions to the K shell are forbidden for $3d$ and $4s$ electrons. This fact can be accounted for by the strong admixing of p states into the occupied-band structure that is implied by $n_{2u}=3$.

(c) If $n_{2u}=3$, nontransition elements with occupied s and p orbitals ($n_{sp}'\sim 3-4$, where primed symbols always refer to solute atoms) should have the largest solid solubility in the bcc phase. The range of solid solubility is limited in most bcc transition elements because of the stability of the $A15$ structure. Since iron does not stabilize the $A15$ structure,[22] it provides the most interesting case study, and the solid solubility of the elements in α Fe is presented in Table III. Given $n_{2u}=3$, the predicted characteristics indicated for the phase diagram, size effects neglected, can be immediately obtained. (i) With one or two outer solute electrons, phase stability is determined by the radius of the closed-shell core. (ii) With three or four outer s and p electrons, the solute readily participates in the $s-p$ band of the α phase, but it has too many electrons for the s band of the γ phase. Therefore, the α phase is favored provided there are three or fewer solute d electrons to participate in the t_{2g} band. With more than three d electrons on the solute, phase stability is largely determined by the magnetic energy, the α phase

[20] J. H. E. Griffiths, Nature **158**, 670 (1946).
[21] A. F. Kip and R. D. Arnold, Phys. Rev. **75**, 1556 (1949).

[22] In the $A15$ structure, formula M_3S', the transition-element atoms M form linear chains suggestive of strong linear bonding via $(d_zp_z)^2\sigma$ bonds and $d^4\pi$ bonds. This suggestion is supported by the observation of an $A15$ structure only with M atoms having four to six outer electrons.

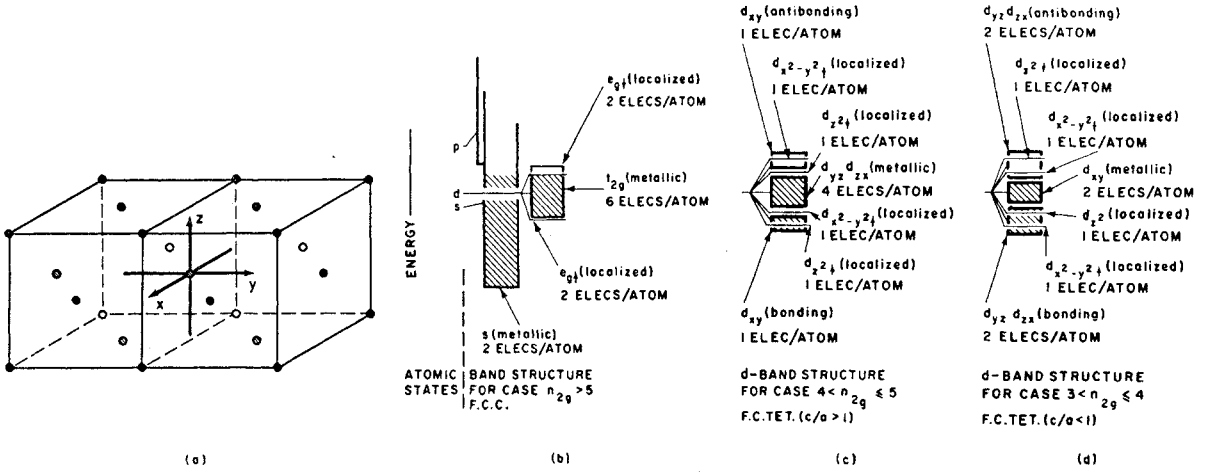

FIG. 3. Qualitative features of band structure for face-centered transition metals of the first long period.

being favored if the average atomic moment $\bar{\mu}$ is increased, the γ phase if $\bar{\mu}$ is decreased. (iii) Solute atoms with five outer s and p electrons, though stabilizing the α vs the γ phase, are essentially donors, and therefore relatively insoluble, if $s-p$ stabilization is due to bonding-band formation. Solutes with six or seven outer s and p electrons are nonmetallic and insoluble unless sufficiently small to enter interstitially. It therefore appears significant that the nontransition elements of greatest solid solubility in α Fe are Al and Si, and this in spite of the fact that Si crystallizes in an extremely stable diamond structure because both its s and p electrons are active in bonding.

(d) Direct measurements of the number of $3d$ electrons in α Fe are compatible with $n_d=5$ (see Sec. IVD).

C. Face-Centered-Cubic Structure

The Cartesian reference frame may be reasonably placed into the fcc structure either as in Fig. 3(a) or as in Fig. 4(a). It is immediately obvious that Fig. 4(a) has tetragonal, not cubic, symmetry. Cubic symmetry is only achieved by a transformation to bcc symmetry via a simultaneous reduction in the separation of (001) planes and an expansion within these planes. This relationship between the fcc and bcc phases was first pointed out by Bain.[23] It is suggested that the driving force for the bcc$\rightleftharpoons$fcc martensitic phase changes comes from the changes in band structure associated with a 45° rotation of the Cartesian reference frame.

In fcc Ni and Co, $R(\text{n.n.n.})\approx 3.5\text{ A}>R_c$ and $R(\text{n.n.})\approx 2.5\text{ A}<R_c$. Further, nearest-neighbor antiferromagnetic order cannot be propagated throughout the structure. It follows that the t_{2g} electrons form a metallic band, that the e_g electrons are localized and form two subbands split by intra-atomic exchange (Hund's rule). The less stable e_g subband is probably overlapped by the t_{2g} band since the repulsion between filled orbitals is smaller for next-near-neighbor than for near-neighbor-directed orbitals. The relative stabilities of $E_b(2g)$ and the more stable e_g subband are much less certain. The exact placement is not crucial for the arguments to follow. In Fig. 3 the lower e_g subband is shown more stable than $E_b(2g)$; this leads to a density-

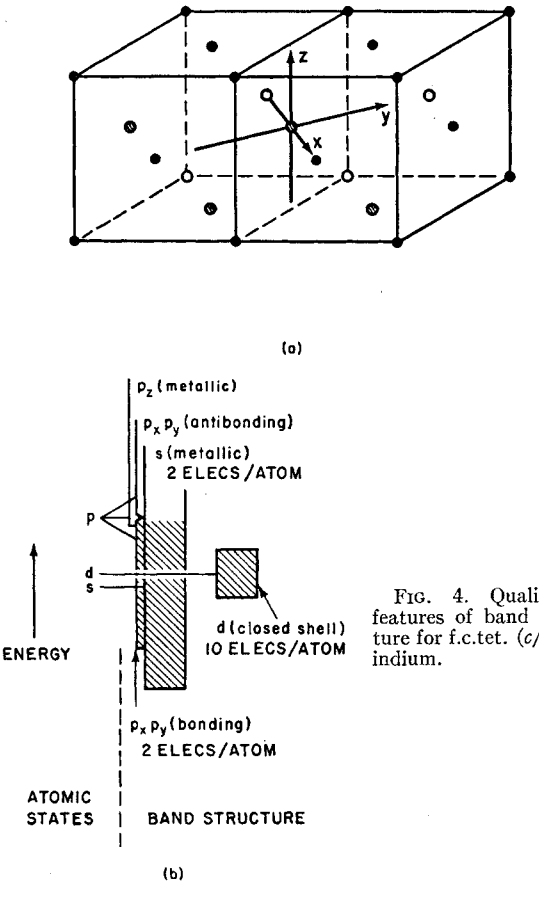

FIG. 4. Qualitative features of band structure for f.c.tet. ($c/a>1$) indium.

[23] E. C. Bain, Trans. Am. Inst. Mining, Met., Petrol. Engrs. **70**, 25 (1954).

of-states curve with principal features similar to those of the Krutter[24]-Slater[25] curve for copper. The fcc symmetry is not suitable for bonding-band stabilization of the p orbitals: The number of $s-p$ electrons is therefore $n_s \sim 1$. To provide a model for the first long period that is consistent with experiment, it is necessary to choose $n_s \approx 0.55$, 0.75, 0.95, 1.15, respectively,[26] for Ni, Co, Fe, Mn.

Since bonding-band stabilization should occur whenever possible, the fcc structure can only be stable to lowest temperatures if $n_{2g}=0$ or $5<n_{2g}\leqslant 6$. If $4<n_{2g}\leqslant 5$ or $3<n_{2g}\leqslant 4$, for example, there are one or two t_{2g} holes, respectively, that can order among the t_{2g} electrons. One hole would order into the d_{xy} orbitals to permit formation of a bonding d_{xy} band, two holes would order into d_{yz}, d_{zx} orbitals. Such ordering would be accompanied by a cooperative lattice distortion to tetragonal symmetry: in the former case $c/a>1$, in the latter $c/a<1$. Such ordering would also introduce antiferromagnetic order: in the former case antiferromagnetic coupling within (001) planes, in the latter between (001) planes. If $2<n_{2g}\leqslant 3$, the Cartesian reference frame is rotated 45° to permit formation of a bonding t_{2g} band, and a bcc phase is more stable than the fcc phase.

Before closing this discussion, it seems relevant to suggest that the tetragonal ($c/a=1.076$) symmetry of metallic indium is due to electron ordering that forms a bonding (p_xp_y) band, the Cartesian reference frame being oriented as shown in Fig. 4(a). The associated band structure is pictured in Fig. 4(b).

D. Close-Packed-Hexagonal Structure

The most reasonable configuration for the Cartesian reference frame in a c.p.h. lattice has the z axis parallel to the c axis. Nearest-neighbor antiferromagnetic order cannot be propagated throughout the structure unless $c/a<1.63$. Since hybridized (pd^5) orbitals are directed toward the six near neighbors in adjacent planes, bonding-band formation with $c/a<1.63$ is possible provided the separation of atomic d and p states is small (perhaps second and third long periods). Figure 5(a)-(b) shows the qualitative features of the c.p.h. band structure (a) without and (b) with (pd^5)-bonding-band formation. It is immediately seen that if there are more than eight outer electrons, the c.p.h. structure is either metallic or rendered less stable by the presence of occupied antibonding states. It follows that in c.p.h. Co and Ni, the d_{z^2} electrons may be localized and capable of providing an atomic moment while the other d electrons are metallic. Therefore, if the d_{z^2} orbitals are full (as is probable for Ni), there is no spontaneous magnetization; but if they are partially filled (as is probable for Co), there may be a spontaneous magnetization equivalent to the total number of holes in the more than half-filled d bands.

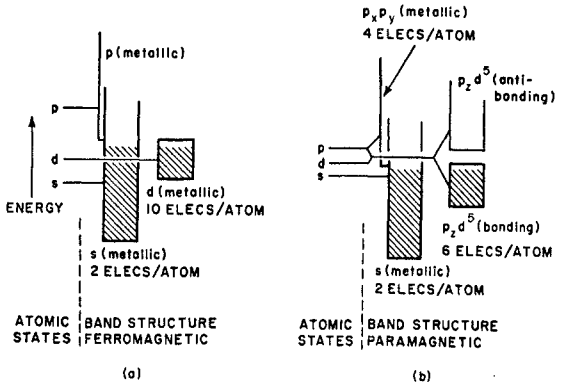

FIG. 5. Qualitative features of band structure for c.p.h. transition metals: (a) relatively large separation of atomic p and d states (e.g., cobalt) and (b) relatively small separation of atomic p and d states and ≤ 8 outer electrons.

III. SEMIEMPIRICAL DENSITY-OF-STATES CURVES

In order to obtain more quantitative density-of-states curves, it is assumed that the major peaks and valleys of such a curve are described by a knowledge of the relative widths and positions of the individual bands and subbands. Therefore, the detailed configurations are ignored, and a simple parabolic-energy-band approximation $\delta E_i = a_i[n(\delta E_i)]^2$ is assumed for both the electrons at the bottom and the holes at the top of the bands. Only in the case of the t_{2g} band is it necessary to assume a bimodal character for the band. In order to construct easily calculable curves that permit contact with experiment, numbers are chosen for the individual a_i that provide the most consistent interpretation of available information. From a knowledge of the total number of electrons, or holes, in an energy interval ΔE_i, it is possible to calculate a_i from the relation

$$n_i = \int_0^{\Delta E_i} n(\delta E)d(\delta E) = \frac{2(\Delta E_i)^{\frac{3}{2}}}{3a_i^{\frac{1}{2}}} = \tfrac{2}{3}\Delta E_i n(\Delta E_i).$$

To obtain a quantitative relationship between n_i and ΔE_i, use is made of available electronic-specific-heat data (see Table III). With the aid of Fermi statistics and the assumption that $kT \ll E_F$, where E_F is the Fermi energy, it is possible to show[27] that the electronic specific heat for a paramagnetic metal with a single conduction band is

$$C_{el} = \gamma_{el} T; \quad \gamma_{el} \approx \tfrac{1}{3}\pi^2 k^2 n(E_F).$$

If there is more than one conduction band and the metal has a net magnetization, the expression for γ_{el} becomes more complicated.[28] However, in rough

[24] H. M. Krutter, Phys. Rev. 48, 664 (1935).
[25] J. C. Slater, J. Appl. Phys. 8, 385 (1937).
[26] Refer to Sec. IVB for justification of these numbers from magnetic data.
[27] F. Seitz, *The Modern Theory of Solids* (McGraw-Hill Book Company, New York, 1940), p. 151.
[28] E. P. Wohlfarth, Proc. Roy. Soc. (London) **A195**, 434 (1949).

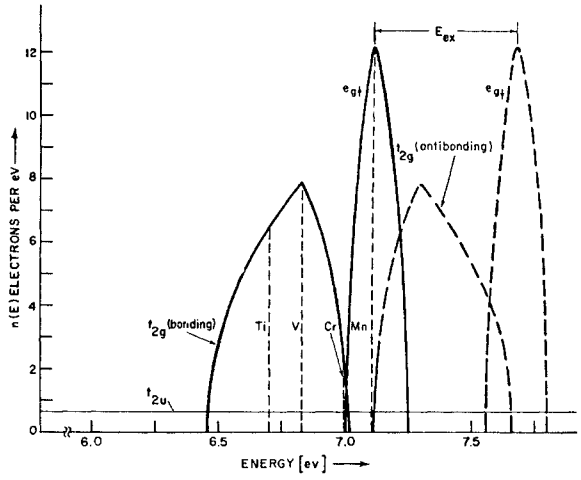

FIG. 6. Simplified density of states for chromium. Energy scale is referred to bottom of t_{2u} band. The Fermi level relative to the d bands is also shown for bcc Ti, V, and Mn. Ferromagnetic, simple-cubic sublattices are coupled antiferromagnetically.

approximation

$$\gamma_{el}\sim 1.7\times 10^{-4}\Sigma_i n_i(E_F) \text{ cal/mole deg}^2,$$

where the $n_i(E_F)$ are the densities of states (in units of ev^{-1}) at the Fermi surface for the various partially filled bands.

It has already been pointed out that in the bcc structure it is necessary to choose $n_{2u}\approx 3$. The positive Hall constant[29,30] and small atomic moment ($\sim 0.4\mu_B$/atom)[31] of Cr indicate a small overlap of the bonding t_{2g} subband and the lower e_g subband. The numbers $n_g\approx 0.01$ and $n_{2g}\approx 2.99$ were chosen since $10^4\gamma_{el}=3.8$ cal/mole deg^2 is small. With the relative positions of the bands fixed, it is only necessary to have $10^4\gamma_{el}=15$, 22.5 for bcc V and Mn, respectively,[32] and $\Delta E_{2u}=7$ ev from x-ray absorption data[33] to estimate the widths of the bands. Since V has a positive Hall constant, $a_{2g}{}^{(t)}/a_{2g}{}^{(b)}=\frac{1}{2}$ gives the broadest possible t_{2g} band. For the narrower e_g band, the ratio $a_g{}^{(t)}/a_g{}^{(b)}=1$ is taken. Straightforward calculations then give Fig. 6. There may be no discrete energy gap in the t_{2g} band in the case of Ti, V, and paramagnetic Cr and δMn. However, a deep minimum at the energy of symmetry effectively splits the band into its bonding and antibonding components.

In the case of ferromagnetic iron, it is necessary to consider two separate sublattices in order to properly account for the electron correlation between the ferromagnetic e_g and t_{2g} electrons. In Fig. 7 the relative bandwidths of Fig. 6 have been used for the construction of the bonding portion of the t_{2g} band, the e_g bands, and the t_{2u} band. The absolute scale comes from x-ray absorption measurements that indicate $\Delta E_{2u}=5$ ev.[33] Perfect electron correlation implies that the principal contribution to the electronic specific heat comes from the antibonding t_{2g} electrons, and the width of the antibonding band is estimated from the datum[32] $\gamma_{el}=12\times 10^{-4}$ cal/mole deg^2.

Construction of a semiempirical density-of-states curve for the fcc elements requires more experimental information than is currently available. For pure nickel[32–36] $\mu_{Ni}=0.604\mu_B$, $g_{Ni}=2.193$, $10^4\gamma_{el}=17.4$ cal/mole deg^2, total occupied bandwidth is 5 ev, and the ratio of e_g to t_{2g} holes is 1:3. Recent measurements[37] of γ_{el} for Ni-Co alloys indicate that γ_{el} is a maximum for

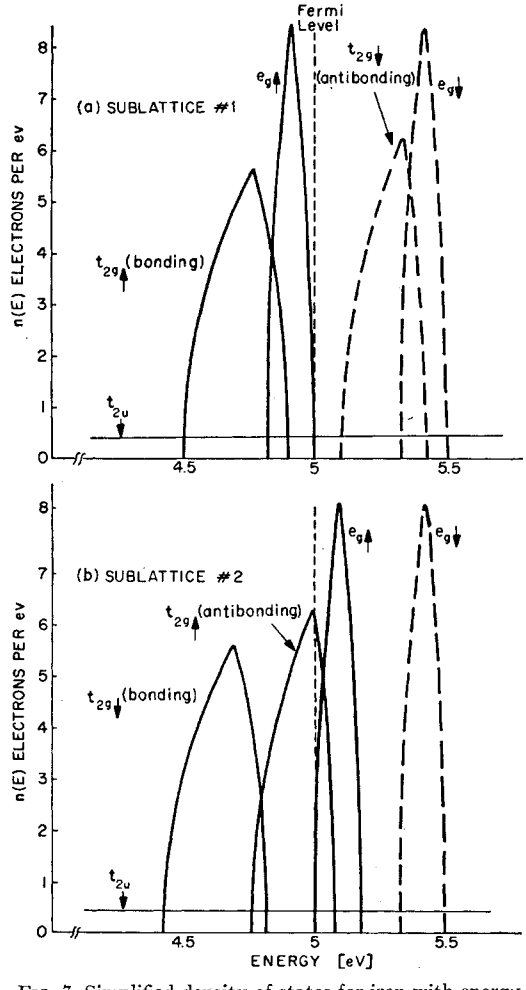

FIG. 7. Simplified density of states for iron with energy scale referred to bottom of t_{2u} band.

[29] S. Foner, Phys. Rev. **107**, 1513 (1957).
[30] G. DeVries and G. W. Rathenau, J. Phys. Chem. Solids **2**, 339 (1957).
[31] C. G. Shull and M. K. Wilkinson, Revs. Modern Phys. **25**, 100 (1953).
[32] M. Horowitz and J. G. Daunt, Phys. Rev. **91**, 1099 (1953).
[33] W. Hume Rothery and B. R. Coles in *Advances in Physics*, edited by N. F. Mott, C. Taylor and Francis, Ltd., London, 1954), Vol. 3, p. 149.
[34] R. M. Bozorth, in *American Institute of Physics Handbook* (McGraw-Hill Book Company, New York, 1957), p. 5-208.
[35] A. J. P. Meyer, Compt. rend. **246**, 1517 (1958).
[36] R. Nathans and A. Paoletti, Phys. Rev. Letters **2**, 254 (1959).
[37] J. C. Walling and P. B. Bunn, Proc. Roy. Soc. (London) **74**, 417 (1959).

pure nickel. Since the e_g electrons of the fcc structure are localized and therefore nonconducting,[10] they probably do not contribute to γ_{el}, so that the maximum $n(E)$ for the t_{2g} band seems to occur at Ni with $\mu_{Ni}/(\frac{1}{2}g_{Ni})=0.55$ $3d$-band holes, or 0.41 t_{2g} holes and 0.14 e_g holes. This gives $a_{2g}{}^{(t)}/a_{2g}{}^{(b)}=\frac{1}{6}$ for the top of the t_{2g} band. Form-factor studies[36] of fcc Co by means of a polarized-neutron beam suggest a ratio of e_g to t_{2g} holes of 1.29:0.43. Theoretically, this fixes the relative widths and positions of the upper e_g subband and the top of the t_{2g} band.[38] The bottom half of the t_{2g} band is assumed symmetrical with the top half; the lower e_g subband is arbitrarily placed just below $E_b(2g)$. The resulting curves are shown in Fig. 8. Admixture of degenerate e_g and t_{2g} states must alter the curves in an energy interval that includes the upper e_g subband.

Figures 6–8 are obviously rough estimates representing averaged density-of-states curves that reflect the thought process of considering successive problems, each with a larger electron/atom ratio than the former. The construction of these semiempirical curves has been consistent with the qualitative predictions that followed from the original postulates. Further, the empirical data used were γ_{el} for V, Cr, Mn, Fe, and Ni; the atomic moment of Cr, Fe, Co, and Ni; polarized-neutron form-factor data for fcc Co and Ni; and soft x-ray data. The positive Hall constant for Cr was noted to be consistent with a nearly filled, bonding t_{2g} subband. There now remains the task of applying these curves and concepts to a variety of other band-structure-dependent physical properties.

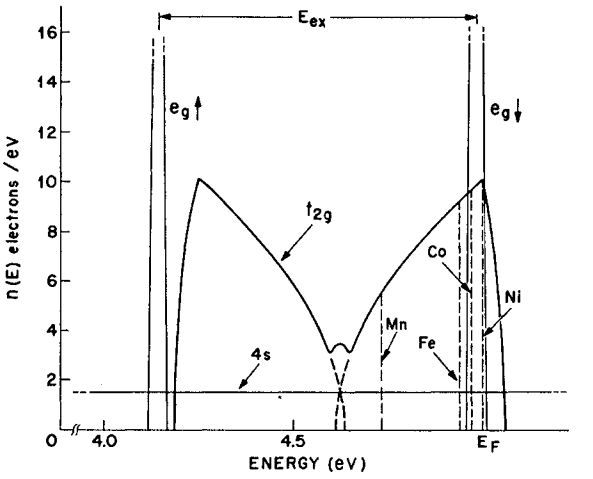

FIG. 8. Schematic density-of-states curve for fcc nickel as suggested by polarized-neutron experiments. $n(E)$ for $4s$ band is enlarged by a factor of ten. Fermi level E_F is 5 ev above bottom of $4s$ band.

IV. COMPARISON WITH EXPERIMENT

A. Crystal Structures

In a pure metal, all of the atoms are identical and there is no Madelung energy so that phase stability is determined by the character of the electron energy bands. The various metallic phases found in the first three long periods are given in Table II.

With one outer electron in an s band, there is little energy difference between bcc and close-packed phases from Brillouin-zone considerations. Some bonding-band stabilization is possible in the bcc structure, but a strong interaction of inner cores, e.g., $3d$ cores of the IB metals, favors a close-packed phase.[39]

With a larger number of outer electrons, simple Brillouin-zone considerations are complicated by interactions between the Fermi surface and the Brillouin-zone surface, and are rendered inapplicable if a large fraction of the outer electrons are located outside of the first zone. Although it is not possible to predict the relative stabilities of the c.p.h. vs fcc phase from the present qualitative considerations, in the c.p.h. phases with eight or fewer outer electrons/atom, a $c/a<1.63$ and an increasing melting point with increasing electron/atom ratio is consistent with stabilization via (pd^5) bonding-band formation. In the fcc phase no such stabilization is possible. The change from c.p.h. to fcc on going from Column VIIIA to VIIIB in the second and third long periods is also suggestive that (pd^5)-band formation is important for these periods. Given the fcc phase, the more than half-filled, metallic t_{2g} bands should contribute to the binding energy, but with decreasing amounts as they become more nearly filled. This prediction is consistent with the melting points found in Columns VIIIB, VIIIC, IB.

More important for the arguments of this paper is the occurrence of the bcc structure in Columns IVA, VA, VIA. From Figs. 2 and 6 it follows that the most stable bcc configuration should occur in VIA with six bonding t_{2g} and t_{2u} electrons. Additional electrons must occupy antibonding e_g states and therefore reduce the melting point of the bcc phase. This prediction is consistent with Table II since evidence for a few e_g electrons first appears in Cr, but not yet in Mo and W, and a reduced melting point, noted in Cr, is marked for δMn. The relative instability of the bcc phase in Column VII is also evidenced by the occurrence of alternate phases. That the melting point of α Fe is not consistently below that of δMn is not necessarily inconsistent with these arguments since the band structure of bcc Fe is somewhat modified by the presence of "extra" t_{2g} electrons (as pointed out, next-near-neighbor e_g-t_{2g} correlations are possible) and the magnetic energy is playing a role.

Manganese is famous for its peculiar structures. With $n_s\approx1.15$, it follows from Fig. 8 that $3<n_{2g}<4$ in γ Mn, and therefore that below some critical temperature t_{2g}-hole ordering should induce a martensitic fcc⇌f.c.tet. $(c/a<1)$ transformation. The existence of

[38] However, the accuracy of the form-factor data and its interpretation are not sufficient to reliably establish the width of the narrow e_g subband.

[39] N. F. Mott and H. Jones, *Theory of the Properties of Metals and Alloys* (Oxford University Press, New York, 1936), Chap. V.

TABLE II. Some physical properties of elements of the first three long periods of the periodic table. $R_0[10^{-13}$ v cm/amp gauss$]$ = ordinary Hall constant[a]; $\gamma_{el}[10^{-4}$ cal/mole deg$^2]$ = electronic-specific-heat constant,[b,c,d] dx/dt = rate of change of paramagnetic susceptibility with temp.[e] Atomic magnetic moments expressed in Bohr magnetons per atom[b]; data on manganese[d]; data on strontium[f]; phase boundaries for Ti,[g] for all others,[h] melting points.[i] Axial ratio c/a for c.p.h. structures are given in parentheses. Stability ranges for each phase are given below the phase identification.

IA (s^1)	IIA (s^2)	IIIA (d^1s^2)	IVA (d^2s^2)	VA (d^3s^2) (d^4s^1)	VIA (d^5s^1) (d^4s^2)	VIIA (d^5s^2) (d^6s^1)		VIIIA (d^6s^2) (d^7s^1)		VIII B (d^7s^2) (d^8s^1)	VIII C (d^8s^2) (d^{10}) (d^9s^1)	IB ($d^{10}s^1$)
K	Ca	Sc	Ti	V	Cr	Mn		Fe		Co	Ni	Cu
bcc	fcc	cph(1.585-8)	cph(1.587)	bcc	bcc	α : A_{12}	γ: fc tet $\rightleftharpoons$ fcc	α : bcc	γ fcc	cph(1.623)	fcc	fcc
0-336°K	0-723°K	0 - ? °K	0-1153°K	0-2190°K	0-2176°K	0-1000°K	1364 - 1410°K	0-979°K	979 - 1674°K	0 - 723°K	0-1728°K	0 - 1356°K
	γ_{el} = 2.9		γ_{el} = 8.0	γ_{el} = 15(22.2)	γ_{el} = 3.8	γ_{el} = 42	γ_{el} = 11.2	γ_{el} = 12.0	↑↓:(?)	γ_{el} = 12.0	γ_{el} = 17.4	γ_{el} = 1.6 - 1.8
		fcc	dx/dt > 0	dx/dt < 0	dx/dt > 0	↑↓:COMPLEX	↑↓: 2.3 μ_B	↑↓: 2.22 μ_B		↑↓: 1.72 μ_B	↑↓: 0.6 μ_B	
	cph(1.63)	? - 1673 °K		R_0 = +8.20	↑↓: ~0.4 μ_B	β : A_{13}	δ : bcc	R_0 = +2.45	δ : bcc	R_0 = -13.3		
	723-1123°K		bcc		R_0 = +36.3	1000 - 1364°K	1410 - 1517°K		1674 - 1812°K	fcc		
			1153 - 1950°K			PARAMAG (?)	γ_{el} = 22.5			723 - 1768°K		
							↑↓: ~ 1 μ_B			↑↓: 1.75 μ_B		
Rb	Sr	Y	Zr	Nb	Mo	Tc		Ru		Rh	Pd	Ag
bcc	fcc	cph(1.585-8)	cph(1.592)	bcc	bcc	cph (1.604)		cph (1.583)		fcc	fcc	fcc
0-312°K	0 - 488°K	0-1773°K	0 - 1140°K	0 - 2770°K	0 - 2890°K	0 - 2408°K		0 - 2700°K		0 - 2239°K	0-1828°K	0 - 1234°K
	cph(1.63)		γ_{el} = 6.92(3.92)	γ_{el} = 17.5 - 20.4	γ_{el} = 5.1			γ_{el} = 8.0		γ_{el} = 10 - 11.7	γ_{el} = 31.0	γ_{el} = 1.45 - 1.6
	488 - 878°K		dx/dt > 0	dx/dt < 0	dx/dt > 0			dx/dt > 0		dx/dt > 0	dx/dt < 0	
	bcc		bcc									
	878 - 1043°K		1140 - 2125°K									
Cs	Ba	La	Hf	Ta	W	Re		Os		Ir	Pt	Au
bcc	bcc	cph(1.61)	cph (1.587)	bcc	bcc	cph (1.615)		cph (1.579)		fcc	fcc	fcc
0-302°K	0-983°K	0 - 1644°K	0-2250°K	0 - 3270°K	0 - 3650°K	0 - 3453°K		0 - 3000°K		0 - 2727°K	0-2043°K	0 - 1336°K
		γ_{el} = 16 - 21	γ_{el} = 6.3 - 6.8	γ_{el} = 13.0 - 14.0	γ_{el} = 1.8 - 2.5	γ_{el} = 5.85		γ_{el} = 5.62		γ_{el} = 7.5 - 7.6	γ_{el} = 16.0	γ_{el} = 1.67
			dx/dt > 0	dx/dt < 0	dx/dt > 0	dx/dt < 0		dx/dt > 0		dx/dt > 0	dx/dt < 0	

[a] S. Foner, Phys. Rev. **107**, 1513 (1957).
[b] *American Institute of Physics Handbook* (McGraw-Hill Book Company, New York, 1957).
[c] M. Horowitz and J. G. Daunt, Phys. Rev. **91**, 1099 (1953).
[d] R. J. Weiss and K. J. Tauer, J. Phys. Chem. Solids **4**, 135 (1958).
[e] C. J. Kriessman and H. B. Callen, Phys. Rev. **94**, 837 (1954).
[f] E. A. Sheldon and A. J. King, Acta Cryst. **6**, 100 (1953).
[g] A. D. McQuillan and M. K. McQuillan, *Metallurgy of the Rare Metals* (Butterworths Scientific Publications, Ltd., London, 1956).
[h] H. H. Landolt and R. Börnstein, *Zahlenwerte und Funktiones aus Physik Chemie Astronomie Geophysik und Technik* (Springer-Verlag, Berlin, 1955).
[i] D. R. Stull and G. C. Sinke, "Thermodynamic Properties of the Elements," A.C.S. #18 (1956).

such a transformation and the magnetic properties of the low-temperature phase can be extrapolated from Mn-rich Mn-Cu alloys.[40,41] Further, if this explanation for the phase transformation is correct, the transformation temperature would drop with added Cu as observed[41] since Cu, with a full $3d$ shell, cannot be stabilized by a distortion that splits the t_{2g} levels.

The solubilities of the various elements in α Fe shown in Table III have already been discussed. [See Sec. IIB, paragraph (c)].

B. Magnetic Properties

One of the important claims for the model presented here is that it provides a sharp criterion for the existence of Pauli paramagnetism, antiferromagnetism, ferromagnetism, or ferrimagnetism. It is shown below that the model is not only successful in this respect, but also as a guide for predictions of the type of magnetic order to be found in ferrimagnetic and antiferromagnetic systems. It is further shown that despite the qualitative nature of the model, it enables predictions of the magnitudes of the individual atomic moments to within a fraction of a Bohr magneton.

1. Body-Centered-Cubic Metals and Alloys

a. Elements. From Figs. 2 and 6, it follows that if $n_{2g} \leqslant 3$ and $n_g = 0$, there are no localized electrons present and only Pauli paramagnetism can exist. With $n_{2u} \approx 3$, the transition from Pauli paramagnetism to antiferromagnetism must occur at, or just beyond, Column VIA. The magnetic properties of the elements

[40] D. Meneghetti and S. S. Sidhu, Phys. Rev. **105**, 130 (1957).
[41] G. E. Bacon, I. W. Dunmur, J. H. Smith, and R. Street, Proc. Roy. Soc. (London) **A241**, 223 (1957).

are indicated in Table II, and Pauli paramagnetism is found in Columns IVA, VA, and VIA with the exception of Cr, which is antiferromagnetic with a small ($\sim 0.4\mu_B$) atomic moment. That Cr is just at the transition to antiferromagnetism is suggested not only by its low atomic moment, but also by its complex magnetic order,[42–44] by its temperature-independent susceptibility,[45] and the sensitivity of its Néel point to impurities.[46] Kriessman and Callen[47] have argued that the rate of change with temperature of Pauli-paramagnetic susceptibility should be $d\chi/dT>0$ if E_F is near a minimum in the density-of-states curve, $d\chi/dT<0$ if E_F is near a maximum. Comparison of Fig. 6 with Table II shows consistency with this argument. Further, consistency demands that if Cr is antiferromagnetic, then δ Mn and the bcc Cr-Mn alloys are antiferromagnetic and that the atomic moments are $(n_g+\delta_{2g})\mu_B$, where δ_{2g} is the localization of the t_{2g} electrons induced via intra-atomic exchange by the presence of e_g electrons. From the moment of Cr it appears that $\delta_{2g}\sim 0.3$. Therefore, from Fig. 6 it follows that δ Mn has an atomic moment $\mu_{\mathrm{Mn}}\approx 1.3\mu_B$. Neutron-diffraction measurements[48] of disordered MnCr confirm the predicted antiferromagnetic coupling between the simple-cubic sublattices and a $\bar{\mu}=(0.85\pm 0.04)\mu_B$ as compared with a predicted $\bar{\mu}=(\mu_{\mathrm{Mn}}+\mu_{\mathrm{Cr}})/2=0.85\mu_B$.

If $n_{2u}\approx 3$, consistency requires that the transition from antiferromagnetism to ferromagnetism occur at or before α Fe since Fe has 8 outer electrons. Whereas the atomic moment of antiferromagnetic iron would be $(2+\delta_{2g})\approx 2.3\mu_B$, the atomic moment of ferromagnetic iron is slightly smaller (as discussed above) since the bonding t_{2g} electrons do not contribute.

Thus granted $n_{2u}\approx 3$ for all the bcc transition elements, there follows a consistent interpretation of the type of magnetism and the magnitude of the atomic moments for the bcc elements. There remains to inquire whether the model is applicable to other bcc alloys than MnCr.

b. Alloys. The measured and predicted magnetic properties of the bcc Fe alloys are listed in Table III. The predicted moments follow from the fact that the model distinguishes four types of solute atom: (1) those with only outer s and p electrons (nontransition elements), (2) those with $n_{2g}'\leqslant 3$, $n_g'=0$ (Columns IVA, VA, VIA except Cr), (3) those with $n_{2g}'\leqslant 3$, $n_g'>0$ (Cr, Mn, and probably Tc and Re), and (4) those with $3<n_{2g}'<6$, $n_g'<4$ (Columns VIIIA, VIIIB, VIIIC).[49]

With no d electrons, solute atoms of type (1) carry no moment so that the rate of change of average magnetization with solute concentration c is simply $d\bar{\mu}/dc=-(2.2+\Delta n_{2u}{}^{\mathrm{Fe}})\mu_B\approx -2.2\mu_B$, where $\Delta n_{2u}{}^{\mathrm{Fe}}$ is a measure of any small relative shift of the t_{2u} bands with c. The most important type (1) solutes are Al and Si. These form the ordered alloys FeAl, Fe_3Al, and Fe_3Si. Since Al has no d electrons, no t_{2g} band can be formed in the CsCl-type FeAl. However, $R(\mathrm{n.n.n.})\approx R_c$ so that a bonding e_g band can be formed of the Fe sublattice. This introduces antiferromagnetic order on the Fe sublattice with $\mu_{\mathrm{Fe}}=(n_{2g}+\delta_g)\mu_B$. If $n_{2u}\approx 3$, this would mean $\mu^{\mathrm{Fe}}\approx 3\mu_B$.[50] Ordered Fe_3Al and Fe_3Si, on the other hand, carry two types of iron atoms: $\mathrm{Fe_I}$ occupies an ordered rocksalt-type Fe-Al sublattice and $\mathrm{Fe_{II}}$ occupies an all-Fe, simple-cubic sublattice.[51] The $\mathrm{Fe_I}$ atom, with all Fe nearest neighbors, should have an atomic moment $\mu_{\mathrm{FeI}}=(2.2+\Delta n_{2u}{}^{\mathrm{FeI}})\mu_B\approx 2.2\mu_B$. The $\mathrm{Fe_{II}}$ atom, with four tetrahedral nearest-neighbor Fe atoms and four similar Al atoms, may experience a larger Δn_{2u} and therefore have a somewhat lower moment. However, another mechanism is expected to be present to lower the apparent μ_{FeII}. There must be some critical number of Al nearest neighbors, $n_{\mathrm{Al}}{}^c$ where $4<n_{\mathrm{Al}}{}^c<8$, at which e_g bonding with next-nearest-neighbors $\mathrm{Fe_{II}}$ is more stable than t_{2g} bonding with nearest neighbor $\mathrm{Fe_I}$. If $n_{\mathrm{Al}}{}^c=5$, then $\bar{\mu}_{\mathrm{FeII}}\approx[2.2(1-4x)-12x]\mu_B \approx(2.2-21x)\mu_B$, where x is the fraction of $\mathrm{Fe_I}$ atoms that are disordered. To obtain the observed $\bar{\mu}$ for the ordered alloys, it is necessary to assume $x\approx 0.035$ for Fe_3Al ($\bar{\mu}_{\mathrm{FeI}}=(2.14\pm 0.1)\mu_B$, $\bar{\mu}_{\mathrm{FeII}}=(1.46\pm 0.1)\mu_B$, $\bar{\mu}_{\mathrm{Al}}=(0.12\pm 0.1)\mu_B$ [52] and $x=0.05$ for Fe_3Si[$\bar{\mu}(Fe_3Si)=1.15\mu_B$].[53] Such a degree of disorder is reasonable.

With $n_g'=0$, solute atoms of type (2) also carry no moment. However, they participate in the bonding t_{2g} band whereas type (1) solutes do not. Thus a CsCl-type alloy with a type (2) solute would, in contrast to FeAl, be ferromagnetic since the bonding t_{2g} band inhibits

[42] J. Hastings, Neutron Diffraction Conference, Gatlinburg, Tennessee, April, 1960 (unpublished).

[43] G. E. Bacon, Neutron Diffraction Conference, Gatlinburg, Tennessee, April, 1960 (unpublished).

[44] M. K. Wilkinson, E. O. Wollan, and W. C. Koehler, Neutron Diffraction Conference, Gatlinburg, Tennessee, April, 1960 (unpublished).

[45] T. R. McGuire, Neutron Diffraction Conference, Gatlinburg, Tennessee, April, 1960 (unpublished).

[46] G. DeVries [J. phys. radium **20**, 428 (1959)] has observed a rapid drop in T_N with small additions of V that extrapolates to $T_N=0°\mathrm{K}$ at ~ 4 atomic percent V, a rapid increase in T_N with small additions of Mn. These observations are compatible with Fig. 6 and E_F(Cr) at the transition to antiferromagnetism.

[47] C. J. Kriessman and H. B. Callen, Phys. Rev. **94**, 837 (1954).

[48] J. S. Kasper and R. M. Waterstrat, Phys. Rev. **109**, 1551 (1958).

[49] Primed symbols always refer to solute.

[50] Similarly ordered CoAl and NiAl are predicted to be antiferromagnetic with $\mu_{\mathrm{Co}}\approx 2\mu_B$, $\mu_{\mathrm{Ni}}\approx 1\mu_B$. However, the electronegativity difference of Al and the transition elements may introduce a larger number of electrons at the transition elements in the ordered phase, thereby reducing these moments considerably.

[51] Such ordering minimizes next-near-neighbor repulsions due to antibonding e_g electrons provided spin correlations order the e_g electrons on $\mathrm{Fe_I}$, the ferromagnetic t_{2g} electrons on $\mathrm{Fe_{II}}$. Evidence that such ordering takes place has been found in recent polarized-neutron-beam experiments [S. J. Pickart and R. Nathans, J. Appl. Phys. Suppl. **31**, 372S (1960)] that suggest (granted the dubious assumption of equal radial distributions of e_g and t_{2g} electrons) that of the magnetic electrons $\sim 70\%$ are e_g on $\mathrm{Fe_I}$ and $\sim 12\%$ on $\mathrm{Fe_{II}}$.

[52] R. Nathans, M. T. Pigott, and C. G. Shull, J. Phys. Chem. Solids **6**, 38 (1958).

[53] R. M. Bozorth, *Ferromagnetism* (D. Van Nostrand and Company, Inc., New York, 1951), pp. 74, 79.

TABLE III. Solid solubility of elements in α Fe and their influence on magnetization of disordered bcc Fe alloys.

Li UNF INS	Be FAV 5-8% CL γ — ($-2.2\mu_B$)	ORDER OF ENTRIES 1. SIZE FACTOR (FAV=FAVORABLE IF WITIN 15% ATOMIC SIZE OF Fe; UNF=UNFAVORALE; MAR=MARGINAL) 2. ATOMIC% SOLID SOLUBILITY IN α Fe. 3. CHARACTERISTICS OF PHASE DIAGRAM (CL γ = CLOSED γ LOOP; γ FAV = γ PHASE FAVORED; NO FAV = NEITHER PHASE FAVORED; INS = INSOLUBLE; INT = INTERSTITIAL) 4. MEASURED RATE OF CHANGE IN MAGNTIZATION PER SOLUTE ATOM OF DISORDERED ALLOY 5. PREDICTED RATE OF CHANGE IN MAGNETIZATION PER SOLUTE ATOM (IN PARENTHESES)										B <0.1% Al MAR 50% ORDER >18% CL γ $-2.3\mu_B$ ($-2.2\mu_B$)	SMALL IONS ENTER INTERSTITIALLY Si FAV 26% ORDER >10% CL γ $-2.2\mu_B$ ($-2.2\mu_B$)	P FAV 1-4% CL γ — ($-2\mu_B$)	S MAR INS	Cl SMALL INS
Na UNF INS	Mg UNF INS															
K UNF INS	Ca UNF INS	Sc UNF — — ($-2.2\mu_B$)	Ti UNF 3-14% CL γ $-3.45\mu_B$ ($<-2.2\mu_B$ & $>-4.2\mu_B$)	V FAV 100% (HIGH T) CL γ $-2.2\mu_B$ ($<-2.2\mu_B$ & $>-3.2\mu_B$)	Cr FAV 100% (HIGH T) CL γ $-2.9\mu_B$ ($<-2.6\mu_B$)	Mn FAV ~10% γ FAV $-2.0\mu_B$(?) ($<-3.5\mu_B$)	Fe	Co FAV 75% NO FAV $1\mu_B$ ($1\mu_B$)	Ni FAV ~8% γ FAV $\sim 0.5\mu_B$ ($>0\mu_B$ & $<2\mu_B$)	Cu FAV <1% γ FAV — ($-2.2\mu_B$)	Zn FAV 3-15% γ FAV — ($-2.2\mu_B$)	Ga FAV α — — ($-2.2\mu_B$)	Ge FAV 18% CL γ — ($-2.2\mu_B$)	As FAV ~8% CL γ — ($-2\mu_B$)	Se FAV INS	Br FAV INS
Rb UNF INS	Sr UNF INS	Y UNF —	Zr UNF INS	Nb UNF <1% α FAV — ($<2.2\mu_B$ & $>-3.2\mu_B$)	Mo FAV 4-20% CL γ — ($-2.2\mu_B$)	Tc —	Ru FAV ~10% γ FAV Max $\bar{\mu}\sim 0$% (Max $\bar{\mu}$ at 0%)	Rh FAV 50% NO FAV $\sim 0.9\mu_B$ ($<1\mu_B$)	Pd FAV ~4% γ FAV $\sim 0\mu_B$ ($>0\mu_B$ & $<2\mu_B$)	Ag MAR INS	Cd UNF INS	In UNF —	Sn UNF 8% CL γ — ($-2.2\mu_B$)	Sb UNF ~5%(?) CL γ — ($-2\mu_B$)	Te MAR INS	I FAV INS
Cs UNF INS	Ba UNF INS	La UNF —	Hf UNF —	Ta UNF <0.5% α FAV — ($<-2.2\mu_B$ & $>-3.2\mu_B$)	W FAV 4% CL γ — ($-2.2\mu_B$)	Re FAV —	Os FAV ~8% γ FAV Max $\bar{\mu}\sim 0$% (Max $\bar{\mu}$ at 0%)	Ir FAV ~12% γ FAV $\sim 0.8\mu_B$ ($<1\mu_B$)	Pt FAV ~10% γ FAV $\sim 2\mu_B$ ($>0\mu_B$ & $<2\mu_B$)	Au MAR <1.5% γ FAV — ($-2.2\mu_B$)	Hg UNF INS	Tl UNF INS	Pb UNF INS	Bi UNF INS	Po UNF INS	At —
PREDICTED CHARACTERISTIC OF PHASE DIAGRAM, NEGLECTING SIZE EFFECTS																
CL γ	CL γ	CL γ	CL γ	CL γ	CL γ	γ FAV	LARGER $\bar{\mu}$ FAVORS α SMALLER $\bar{\mu}$ FAVORS γ		γ FAV	γ FAV	γ FAV	CL γ	CL γ	CL γ	INT OR INS	INT OR INS

[a] Alloys easily. Data from: M. Hansen, *Constitution of Binary Alloys* (McGraw-Hill Book Company, Inc., New York, 1958); R. M. Bozorth, *Ferromagnetism*, D. Van Nostrand Company, Inc., New York, 1951).

formation of e_g bonding.[54] Further,

$$d\bar{\mu}/dc = -(2.2+\Delta n_{2u}{}^{\mathrm{Fe}}+\delta_i')\mu_B,$$

where δ_i' is the number of ferromagnetic t_{2g} electrons of Fe that have been donated to the bonding t_{2g} band. For Ti, $\delta_i' \leqslant 2$; for V, Nb, and Ta, $\delta_i' \leqslant 1$; and for Mo and W, $\delta_i' = 0$. Arrott and Noakes[55] have recently reported $d\bar{\mu}/dc = -3.45\mu_B$ for dilute (<2 atomic percent Ti) Fe-Ti alloys, suggestive of $\delta_i{}^{\mathrm{Ti}} \sim 1.2$.

The type (3) Fe-Cr and Fe-Mn alloys must be more complicated since $n_g' > 0$ and the interactions change from antiferromagnetic to ferromagnetic on passing from Mn to Fe. If charge neutrality prevents "ferromagnetic" t_{2g} electrons from being shared by the solute atoms, it follows that solute-solute interactions are antiferromagnetic, Fe-Fe interactions remain ferromagnetic, and solute-Fe interactions are antiferromagnetic. In this case it follows that for dilute alloys $d\bar{\mu}/dc \approx -(2.2+n_g'+\delta_{2g}')\mu_B$. This appears to be the situation in the Fe-Cr alloys.[56,57] The problem may be more complicated in the Fe-Mn alloys; however, the experimental situation is not clear.[58]

The type (4) solute atoms have ferromagnetic t_{2g} electrons: Therefore, these form ferromagnetic alloys with α Fe. For Column VIIIA solutes, $d\bar{\mu}/dc = -\Delta n_{2u}\mu_B$ is small, where probably $n_{2u}' > 3$ for second- and third-period solutes. Column VIIIB solutes have one additional ferromagnetic electron that can be either t_{2g} or e_g. Therefore, initial additions carry $\mu' \sim 3\mu_B$ so that $d\bar{\mu}/dc \approx 1\mu_B$ (or $d\bar{\mu}/dc < 1\mu_B$ if $n_{2u}' > 3$). However, if the

[54] D. P. Shoemaker, Massachusetts Institute of Technology (unpublished), reports ordered FeV alloys are ferromagnetic.
[55] A. Arrott and J. E. Noakes, J. Appl. Phys. **30S**, 97S (1959).
[56] M. Fallot, Ann. phys. **6**, 304 (1936).
[57] C. G. Shull and M. K. Wilkinson, Phys. Rev. **97**, 304 (1955).
[58] C. Sadron, Ann. phys. **17**, 371 (1932).

electron correlations do not favor ferromagnetic solute t_{2g} electrons, the upper e_g band of a solute is forced to be partially occupied. Such an occupation would reduce μ'. It follows that there is a critical solute concentration c above which $\mu'<3$ unless atomic ordering takes place. The highest concentration with large $\bar{\mu}$ would be a 50–50, ordered compound with $\mu_{Fe}\sim 2.2\mu_B$, $\mu'\sim 3.2\mu_B$, and $\bar{\mu}\sim 2.7\mu_B$. For $c>0.5$, all added solutes would have three e_g electrons and $d\bar{\mu}/dc\approx -1\mu_B$. Measurements[59] of the magnetic properties of the Fe-Co alloys are in substantial agreement with this view. Initially, $d\bar{\mu}/dc\approx 1\mu_B$ and $\bar{\mu}$ reaches a maximum of $2.52\mu_B$ at $c\approx 0.33$. In the compositional range $0.33<c<0.5$ there is evidence of ordering toward a CsCl-type structure, but $\bar{\mu}$ decreases to $2.42\mu_B$ at $c=0.5$. In the ordered alloys, one metal carries $\sim 2.0\mu_B$, the other $\sim 2.9\mu_B$.[60] In the range $c>0.5$, $d\bar{\mu}/dc\approx -1\mu_B$. That the CsCl-type order is never complete is indicated by γ_{el} for the alloys.[61] Above the critical composition $c\approx 0.35$, there is a sharp increase in γ_{el} suggestive of partial filling of the upper e_g subband. With two extra electrons, Column VIIIC solutes can have $\mu'(\max)=(3.5+\delta_{2u})\mu_B$, the maximum t_{2g} magnetization being $1.5\mu_B$/atom, but are likely to have $\mu'\approx(2+\delta_{2u})\mu_B$ since one electron can be expected to occupy the upper e_g band even initially. It follows that $0\mu_B<d\bar{\mu}/dc<2\mu_B$ and that $d\bar{\mu}/dc$ increases with stabilization of the t_{2u}' electrons, or on going from Ni to Pd to Pt.

2. *Close-packed metals and alloys*

a. Elements. It follows from Fig. 5 that the c.p.h. metals are Pauli paramagnetic unless localized, partially filled d_{z^2} orbitals are present. Therefore, the Pauli paramagnetism of the c.p.h. metals containing eight or fewer outer electrons per atom is consistent with a (pd^5) bonding band. The condition for ferromagnetism is that partially filled metallic and localized orbitals be simultaneously present. If this condition is fulfilled, then the atomic moment is $\mu\approx(n_s+m)\mu_B$, where m is 0, 1, 2 for Ni, Co, Fe, respectively.[62] Since the s bands are shallow relative to the d bands, consistency requires that for any element $n_s(\text{c.p.h.})\approx n_s(\text{fcc})$. Consistency also requires that n_s vary more or less regularly on going across any long period.

Magnetization measurements[34,63] of fcc and c.p.h. Co and Ni give $n_s^{Co}(\text{c.p.h.})=0.72\approx n_s^{Co}(\text{fcc})=0.75$ and $n_s^{Ni}(\text{fcc})=0.55$ ($g_{Ni}\neq 2$). At room temperature, c.p.h. Ni is paramagnetic.[64,65] The possibility that c.p.h. Ni be Pauli paramagnetic can be embraced by the present model since the probability that the localized d_{z^2} orbitals are completely filled with more than nine d electrons is high.

Since the $4s$ band becomes increasingly stable relative to the $3d$ band on passing from Ni to Co to Fe to Mn, the estimates $n_s^{Ni}=0.55$, $n_s^{Co}=0.75$ suggest that $1<n_s^{Mn}<2$. As pointed out above, this implies (Postulate III and Fig. 8) a low-temperature, antiferromagnetic phase with f.c.tet. ($c/a<1$) symmetry and ferromagnetic (001) planes alternately antiferromagnetic, reflecting a bonding $(d_{yz}d_{zx})$ band. The f.c.tet.$\rightleftarrows$fcc transition in γ Mn has already been discussed in this connection, but only crystallographically. Further evidence for bonding-band formation below the transition temperature $T_t=T_N$ is found[41] in an anomalous increase of χ with T in a temperature interval above the Néel temperature T_N. Bonding tends to spin-pair some of the d electrons.[13] It therefore follows from Fig. 3(d) that[62] $\mu_{Mn}\approx[2+(n_s^{Mn}-1)+\delta_{yzx}]\mu_B$, where $\delta_{yzx}\sim 0.3$ measures the localization of the $(d_{yz}d_{zx})$ electrons induced by the localized electrons simultaneously present. Neutron-diffraction measurements[40,41] confirm the predicted magnetic order for $T<T_t$ and reveal a $\mu_{Mn}=(2.4\pm 0.1)\mu_B$. This suggests $n_s^{Mn}\approx 1.15$ and therefore the consistent progression: $n_s^{Ni}=0.55$, $n_s^{Co}\approx 0.75$, $n_s^{Fe}\approx 0.95$, $n_s^{Mn}\approx 1.15$.

This fact is important not only because it demonstrates the internal consistency of the model and its power to distinguish between antiferromagnetic, ferromagnetic, and Pauli paramagnetic elements, but also because it has important implications for fcc Fe. If $n_s^{Fe}<1$, γ Fe should be cubic, ferromagnetic, with $\mu_{Fe}\sim 3\mu_B$. However, if $n_s^{Fe}>1$, there can be a low-temperature f.c.tet. ($c/a>1$) phase in which the t_{2g} hole is ordered to give a d_{xy} bonding band. The tetragonal phase would have antiferromagnetic coupling within (001) planes and $1\mu_B<\mu_{Fe}<2\mu_B$. [See Fig. 3(c)]. In either case, the high-temperature phase would be cubic with ferromagnetic Fe-Fe interactions. Wilkinson and Shull[66] have observed evidence of ferromagnetic short-range order persisting through the $\alpha\rightleftarrows\gamma$ transition temperature whereas extrapolation[67] of the low-temperature properties of fcc Fe-Mn alloys suggests antiferromagnetism for pure γ Fe. Also, the low-temperature susceptibility of γ Fe precipitated in Cu has been found to be small and temperature independent.[68]

The Pauli paramagnetism of fcc Rh, Pd, Ir, and Pt is not interpretable from the above arguments unless both e_g subbands are considerably more stable in the second and third long periods than in the first (refer Fig. 8). But even this interpretation would require $n_{2g}^{Ir}<5$, $n_{2g}^{Rh}<5$, and for neither Ir nor Rh is a f.c.tet. phase reported.

[59] P. Weiss and R. Foner, Ann. phys. **12**, 279 (1929).
[60] C. G. Shull (private communication). The experiment was unable to distinguish which moment goes with which atom.
[61] C. T. Wei, C. H. Cheng, and P. A. Beck, Neutron Diffraction Conference, Gatlinburg, Tennessee, April, 1960 (unpublished).
[62] This assumes $g=2$.
[63] J. Crangle, Phil. Mag. **2**, 659 (1957).
[64] G. LeClerc and A. Michel, Compt. rend. **208**, 1583 (1939).
[65] I. Teodorescu and A. Glodeanu, Phys. Rev. Letters **4**, 231 (1960).
[66] M. K. Wilkinson and C. G. Shull, Phys. Rev. **103**, 516 (1956).
[67] P. Weiss, L. Corliss, and J. Hastings (quoted by reference 66).
[68] L. Kaufmann and S. Foner, Lincoln Laboratory, 1958 (unpublished).

TABLE IV. Variations in average atomic moment with concentration of nontransition-element solute in fcc Ni and Co.

SOLVENT \ SOLUTE	Cu, Ag, Au	Zn, Cd	Al, Sc, Ga, In	Si, Ge, Sn	P, As, Sb
$-d\bar{\mu}/d(c\mu_B)$ (theory)[a] fcc Ni	1 + Λ	2 + Λ	3 + Λ	4 + Λ	5 + Λ
$-d\bar{\mu}/d(c\mu_B)$ (theory)[a] fcc Co	2 + Λ	3 + Λ	4 + Λ	5 + Λ	6 + Λ
$-d\bar{\mu}/d(c\mu_B)$ (observed)[b] fcc Ni	Cu:1, Au:~1	Zn:2.0	Al:3.0	Si:4 Sn:4–4.1	Sb:~5
(observed)[b] cph Co			Al:2.4 (?)	Si:5.3	

[a] Theory predicts that only solvent atoms carry a magnetic moment.
[b] C. Sadron, Ann. Phys. **17**, 371 (1932); V. Marian, Ann. Phys. **7**, 459 (1937); T. Farcas, Ann. Phys. **8**, 146 (1937).

b. Class (1) alloys. From the above discussion it follows that close-packed, transition-element solvents are of two classes, ferromagnetic and Pauli paramagnetic. The first class, class (1) solvents, have been more widely investigated magnetically. With localized and metallic orbitals that are partially filled, the close-packed alloys can be successfully discussed with the collective-electron model originally proposed by Stoner[69] and later developed by Stoner[70] and Wohlfarth.[71] If $n_h<3$ is the number of holes in the d bands of a class (1) solvent, v' is the number of outer electrons on a gaseous solute atom, and n_d' is the total number of d electrons on the solute when present in the solvent, then the average number of Bohr magnetons per atom in a ferromagnetic alloy is[72]

$$\begin{aligned}\bar{n}_B&=(1-c)(\mu/\mu_B)+c(\mu'/\mu_B)\\&=(1-c)(n_h+\delta_s)-c(v'-n_g'-n_{2g}'-n_s)\\&\qquad+c\begin{cases}n_g'+n_{2g}'+\delta_s' & \text{for } n_d'\leqslant 5\\ 10-n_g'-n_{2g}'+\delta_s' & \text{for } 5\leqslant n_d'\leqslant 10,\end{cases}\end{aligned}$$

where it is assumed that the orbital angular momentum is completely quenched.[73] If n_{hp}, δ_{sp} refer to the pure solvent, it is reasonable to assume that $(n_{hp}+\delta_{sp})-(n_h+\delta_s)=\Lambda_0 c$, where the proportionality constant Λ_0 is a small fraction, positive or negative, that measures the solute-induced alteration of relative d- and s-band stability. With this assumption, it follows that

$$\bar{\mu}=\bar{n}_B\mu_B=\mu(p)-cn\mu_B, \qquad (1)$$

where $\mu(p)$ is the atomic moment of the pure class (1) solvent, and that

$$-\frac{d\bar{n}_B}{dc}=n=(v'+m+\Lambda)-\begin{cases}2(n_g'+n_{2g}') & \text{for } n_d'\leqslant 5\\ 10 & \text{for } 5\leqslant n_d'\leqslant 10,\end{cases}$$

where $\Lambda=(\Lambda_0+\delta_s-\delta_s')$ and $m=n_h-n_s$ is an integer. The application of Eq. (1) follows immediately provided two factors are explicitly considered: (i) the relative energies of the solvent d bands and the solute d levels, (ii) bonding-band (or bond-formation) stabilization that induces, whenever possible, t_{2g}-hole ordering at low temperatures even if such ordering introduces a distortion of the lattice symmetry (as discussed for f.c.tet. γ Mn). These provisos require the distinction of several situations.

Case (a): $n_g'=n_{2g}'=0$ (nontransition element or ionized solute):

$$d\bar{n}_B/dc=-(v'+m+\Lambda). \qquad (2)$$

The experimental information summarized in Table IV indicates that in most alloys $\Lambda\approx 0$. However, recent measurements[74] suggest that $\Lambda\approx 0.5$ for Al, Si, and Ge in fcc Ni.

If a transition-element solute is in a fcc solvent, then any of the cases (*a*) through (*d*) discussed below may be anticipated. However, consistency requires that there be a continuous change from (*a*) to (*d*) on moving to heavier solute elements in any one long period of the Periodic Table, or on going down any column. Inspection of Table V, in which are given atomic moments compatible with observed variations of $\bar{\mu}$ with c according to Eq. (1), shows that these consistency criteria are everywhere fulfilled, and also that the stability of the solute d levels relative to the solvent Fermi level is consistently greater in fcc Ni alloys than in fcc Co alloys. In binary alloys of case (*a*), all of the moment is associated, presumably, with the solvent atoms.

Case (b): $0<n_d'\leqslant 2$ ($0<n_g'\leqslant 2$, $n_{2g}'=0$):

$$d\bar{n}_B/dc=-(v'+m+\Lambda)+2n_d'. \qquad (3)$$

This situation is differentiated from the more general situation $n_d'\leqslant 5$ because of the explicit assumption in the construction of Figs. 3 and 8 that the lower e_g subband is below the metallic t_{2g} band. The principal relevance of this assumption lies in the fact that the solutes corresponding to case (*b*) have ferromagnetic solute-solute interactions if $n_{2g}'=0$, but antiferromagnetic solute-solute interactions[75] if $0<n_{2g}'<2$.

The measured variations $d\bar{\mu}/dc$ for Ni-Cr and Co-Cr alloys are, respectively,[63,76] $-4.4\mu_B$ and $-6.6\mu_B$. With

[69] E. C. Stoner, Phil. Mag. **15**, 1018 (1933).
[70] E. C. Stoner, Proc. Roy. Soc. (London) **A165**, 372 (1938); **A169**, 339 (1939).
[71] E. P. Wohlfarth, Proc. Roy. Soc. (London) **A195**, 434 (1949).
[72] Generalization of the collective-electron model to allow for small magnetizations of the conduction band, δ_s and δ_s', was first suggested by G. S. Krinchik {Izvest. Akad. Nauk S.S.S.R. Ser. Fiz. **21**, 869 (1957) [translation: Bull. Acad. Sci. U.S.S.R. **21**, 869 (1957)]} as a result of C. Zener's [Phys. Rev. **81**, 440 (1951)] proposed s-d coupling.
[73] This assumption cannot be correct so long as $0<n_{2g}<6$. However, it should not introduce an error greater than ~10% and is therefore neglected in this simplified treatment.
[74] J. Crangle and M. J. C. Martin, Phil. Mag. **4**, 1006 (1959).
[75] It is assumed here that nearest-neighbor solute-solute bond formation occurs even if there is only one n_{2g}' electron. The situation is presumably analogous to Ti_2O_3 in which Ti-Ti d-electron bonding along the c axis is found.[13]
[76] V. Marian, Ann. phys. **7**, 457 (1937).

TABLE V. Interpretation of atomic moments for disordered fcc transition-element alloys. Case (a): Ferromagnetic. Class (1): $\bar{\mu}=\mu(p)-(v'+m+\Lambda)c\mu_B$, $n_d'=0$. Case (b): Ferromagnetic. Class (1): $\bar{\mu}=\mu(p)-(v'+m+\Lambda-2n_{2g}')c\mu_B$, $0<n_d'\leqslant 2$. Case (c): Near-neighbor solute-solute pairs antiferromagnetic. If ferromagnetic (no solute-solute pairs),

$$\text{Class (1)}: \mu=\mu(p)-\left\{v'+m+\Lambda-4-\left[\frac{2n_{2g}'}{6}\right]\right\}c\mu_B, \quad \begin{bmatrix}0<n_{2g}'<3\\ 3\leqslant n_{2g}'\leqslant 5\end{bmatrix}$$

Case (d): Ferromagnetic. Class (1): $\bar{\mu}=\mu(p)-(v'+m+\Lambda-10)c\mu_B$. Class (2): Require sufficient number of ferromagnetic solute-solute pairs to induce ferromagnetism. Symbols: v', v=number of outer electrons of solute, solvent; $m=10-v$, $\mu'(p)$, $\mu(p)$=atomic moment of pure solute, solvent, n_d'=number of solute d electrons; n_{2g}'=number of t_{2g} electrons at solute; $\bar{\mu}$=average atomic moment, and c=concentration of solute; Λ=measure of relative stability of s bands.

v'	4	5	6	7	8	9	10
SOLUTE / SOLVENT	Ti	V	Cr[a]	Mn	Fe	Co	Ni
Ni (m=0) CLASS (1)	CASE (a) $n_S'=4$ $\frac{d\bar{\mu}}{d(c\mu_B)}=\begin{cases}4(\Lambda=0)\\3.8\ (OBS)\end{cases}$	CASE (a) $n_S'=5$ $\frac{d\bar{\mu}}{d(c\mu_B)}=\begin{cases}5(\Lambda=0)\\5.2\ (OBS)\end{cases}$	CASE (b) $n_S'=5.2$ $\mu_{Cr}\approx 0.9\mu_B$ $\mu_{Ni}\approx\left\{\frac{0.6-5.3c}{1-c}\right\}\mu_B$	CASE (c) $n_S'=2.3$ $\mu_{Mn}\approx 4.7\mu_B$ $\mu_{Ni}\approx\left\{\frac{0.6-2.3c}{1-c}\right\}\mu_B$	CASE (d)[b] $n_S'=0.8$ c d	CASE (d) $n_S'=0.79$ $\Lambda=-0.19$ e	CASE (d) $n_S'=0.6$ $\mu_{Ni}=0.6\mu_B$
Co (f.c.c.) (m=1) CLASS (1)	CASE (a) $n_S'=4$ $\frac{d\bar{\mu}}{d(c\mu_B)}=5(\Lambda=0)$	CASE (a) $n_S'=5$ $\frac{d\bar{\mu}}{d(c\mu_B)}=6(\Lambda=0)$	CASE (b) $n_S'=5.8$ $\mu_{Cr}\approx 0.25\mu_B$ $\mu_{Co}\approx\frac{0.75-6.85c}{1-c}\mu_B$	CASE (c) n_S' 4.25 $\mu_{Mn}\approx 2.8\mu_B$ $\mu_{Co}\approx\frac{1.75-5.3c}{1-c}\mu_B$	PROBABLY CASE (d) POSSIBLY CASE (c)	CASE (d) n_S' 0.75 $\mu_{Co}=1.75\mu_B$	
Pd CLASS (2)	CASE (a) PARAMAGNETIC	CASE (b)	CASE (b) or CASE (c)	CASE (c)	CASE (d) $\mu_{Fe}\sim 2.8\mu_B$[f]	CASE (d) $\mu_{Co}\sim 1.7\mu_B$[f]	CASE (d) $\mu_{Ni}\sim 0.6\mu_B$[f]
Pt CLASS (2)	CASE (a) PARAMAGNETIC	CASE (b)	CASE (c) WHERE FERROMAGNETIC $\mu_{Cr}\sim 2.8\mu_B$	CASE (c) WHERE FERROMAGNETIC $\mu_{Mn}\sim 4.7\mu_B$	CASE (d) $\mu_{Fe}\sim 2.8\mu_B$[f]	CASE (d) $\mu_{Co}\sim 1.7\mu_B$[f]	CASE (d) $\mu_{Ni}\sim 0.6\mu_B$[f]

[a] Mo and W ($v'=6$) are Case (a) in Ni with $n_s'=6$, and $d\bar{\mu}/d(c\mu_B)=6$ ($\Lambda=0$) is observed.
[b] Also see Table VI.
[c] $\mu_{Fe}=2.8\mu_B+[(1-c)/c](0.6\mu_B-\mu_{Ni})$, $c<0.33$.
[d] $\mu_{Fe}=2.5\mu_B+[(1-c)/c](0.76\mu_B-\mu_{Ni})$, $0.33<c<0.6$
[e] $\mu_{Co}=1.79\mu_B+[(1-c)/c](0.6\mu_B-\mu_{Ni})$
[f] Assumes concentration of solute-solute pairs sufficiently great to induce spontaneous polarization of t_{2g} band and therefore ferromagnetism. Anticipate $0\mu_B<\bar{\mu}_{Pd}<0.6\mu_B$, $0\mu_B<\bar{\mu}_{Pt}<0.4\mu_B$, the magnitude depending upon the number of solute-solute pairs present.

$\Lambda\approx 0$, this corresponds to $n_d^{Cr}(Ni)=0.8$ and $n_d^{Cr}(Co)=0.2$. [The Co-Cr alloy could also be interpreted as case (a) with $\Lambda=-0.4$]. The linear variation in c for the Ni-Cr alloys holds only for the compositional range $0\leqslant c\leqslant 0.07$, the curve deviating to higher magnetizations for larger c. Such deviations are consistent with a smaller ionization of a Cr atom with a Cr nearest neighbor: They are not consistent with antiferromagnetic Cr-Cr interactions. This supports the arbitrary placement of the lower e_g subband below $E_b(t_{2g})$.

Case (c): $2<n_d'\leqslant 7$: For dilute alloys (no solute-solute n.n. pairs),

$$d\bar{n}_B/dc=-(v'+m+\Lambda)+4+\begin{cases}2n_{2g}' & \text{if } n_{2g}'\leqslant 3\\ 6 & \text{if } n_{2g}'\geqslant 3\end{cases}. \quad (4)$$

With at least one t_{2g} electron or one t_{2g} hole, nearest-neighbor solute-solute bonding can occur so that solute-solute interactions are ferrimagnetic. Therefore the model provides the sharp prediction that *disordered alloys corresponding to case* (c), *as determined from measurements on dilute alloys and Eq.* (4), *must be ferrimagnetic, but without magnetic order, as a result of antiferromagnetic nearest-neighbor solute-solute interactions.*

In the compositional range $0\leqslant c\leqslant 0.08$, $d\bar{n}_B/dc\approx+2.4$ for the Ni-Mn alloys.[76] With $\Lambda\approx 0$, this suggests that $n_d^{Mn}(Ni)=4.7$ and therefore that the Ni-Mn alloys correspond to case (c). Evidence for the resulting ferrimagnetism was first observed in Ni_3Mn, which has $\bar{\mu}\sim 0.3\mu_B$ if disordered, but a large magnetization if ordered (Au_3Cu structure).[77] More recent evidence from magnetization measurements has been reported by Kouvel et al.[78–80] and from neutron-diffraction measurements by Shull and Wilkinson.[57] Although the latter workers report $\bar{\mu}_{Mn}=(3.18\pm 0.25)\mu_B$ in a sample of ordered Ni_3Mn, this is not necessarily in disagreement with $n_d^{Mn}=4.7$ since only 5% disorder would reduce the observed $\bar{\mu}_{Mn}$ from $4.7\mu_B$ to $3.3\mu_B$. Further, more

[77] S. Kaya and A. Kussmann, Z. Physik **72**, 293 (1931).
[78] J. S. Kouvel, C. D. Graham, Jr., and J. J. Becker, J. Appl. Phys. **29**, 518 (1958).
[79] J. S. Kouvel, C. D. Graham, Jr., and I. S. Jacobs, J. phys. radium **20**, 198 (1959).
[80] J. S. Kouvel and C. D. Graham, Jr., J. Phys. Chem. Solids **11**, 220 (1959).

TABLE VI. Atomic moments vs iron concentration c for fcc Fe-Ni alloys.

c		0.257	0.399	0.501
$\frac{\mu_{Fe}}{\mu_B}$	OBSERVED[a]	2.91 ± 0.2	2.72 ± 0.16	2.60 ± 0.1
	THEORY	2.8	2.65	2.65
$\frac{\mu_{Ni}}{\mu_B}$	OBSERVED[a]	0.62 ± 0.02	0.66 ± 0.05	0.67 ± 0.1
	THEORY	0.60	0.66	0.66

[a] C. G. Shull and M. K. Wilkinson, Phys. Rev. **97**, 304 (1955).

recent neutron-diffraction results[81] for ordered NiMn [alternate (001) layers Ni or Mn] give antiferromagnetically coupled Mn atoms within a (001) Mn plane, $\mu_{Mn}=(4.0\pm0.1)\mu_B$, and $\mu_{Ni}\approx0\mu_B$. With a d_{xy} bonding band, the predicted Mn moment for the ordered alloy is $\mu_{Mn}\approx[4.7-(1-\delta_{xy})]\mu_B$, where δ_{xy} is the localization of the bonding electrons induced by the simultaneously present localized electrons. Extrapolation from Cr and δ Mn gives $\delta_{xy}\sim0.3$, or $\mu_{Mn}=4.0\mu_B$. Therefore, $n_d^{Mn}(Ni)\approx4.7$ appears to be correct. From the model it also follows that $\mu_{Ni}\approx0$ for $c>0.26$ (refer Table V).

Crangle[63] reports that fcc Co-Mn alloys have two regions of roughly linear variation of $\bar{\mu}$ with c, one for $c<0.05$ and one for greater c. From the initial slope $d\bar{n}_B/dc=-2.5$ and Eq. (4), it follows that $n_d^{Mn}(Co)=2.75$. Therefore, the Co-Mn alloys must also correspond to case (c), and Co-Mn alloys are predicted to be ferrimagnetic, but without long-range magnetic order, like the Ni-Mn alloys. The Mn atomic moment of Table V is for dilute alloys. The change of slope reported for $c>0.05$ is presumably an indication of antiferromagnetic, nearest-neighbor Mn-Mn interactions.

Case (d): $7<n_d'<10$ $(5<n_{2g}'<6)$:

$$d\bar{n}_B/dc=-(v'+m+\Lambda)+10=\mu'(p)-\mu(p). \quad (5)$$

There can be no solute-solute nearest-neighbor bonding in alloys corresponding to case (d), and therefore all interactions are ferromagnetic. It follows that there can be no sharp discontinuity in $\bar{\mu}$ for ordered vs disordered case (d) alloys.

From Fig. 8 it follows that fcc Co-Ni alloys belong to case (d), and therefore the ferromagnetism of these alloys is in accord with the criteria of the model. Extrapolation to pure Co of the magnetization measurements[82] for fcc Co-Ni alloys gives $\mu(p)_{Co}=1.79\mu_B$, or $\Lambda=-0.19$, as compared with Crangle's[63] extrapolation from high-temperature measurements on pure Co to $\mu(p)_{Co}=1.75\mu_B$.

On the other hand, it is not possible to determine definitely from Fig. 8 whether the fcc Fe-Ni alloys should correspond to case (c) or case (d). The fact that these alloys are ferromagnetic dictates that $n_d^{Fe}>7$, or that $\mu_{Fe}<3$ in these alloys. That this condition is fulfilled has been confirmed by neutron diffraction (see Table VI). Predictions for the individual atomic moments can also be obtained with the aid of Eq. (5) and magnetization measurements. These latter measurements[83] show two linear regions for $\bar{\mu}$ vs c in the range of fcc alloys. In the range $0\leqslant c\leqslant0.33$, the slope is $d\bar{n}_B/dc=2.2\mu_B$ corresponding to an effective $\mu(p')_{Fe}=2.8\mu_B$, $n_d^{Fe}\approx7.2$, and $\Lambda\approx-0.2$. At $FeNi_2$ a rearrangement of the band structure seems to occur, and for $0.33\leqslant c\leqslant0.6$ the effective $\mu(p'')_{Fe}$ and $\mu(p')$ are $2.5\mu_B$ and $0.76\mu_B$ or $d\bar{n}_B/dc=1.74$ corresponding to $\Lambda\approx+0.26$. In Table VI, the resulting atomic moments are compared with experiment.

It should be noted that consistency requires $n_d^{Fe}(Co\text{-}Fe)<n_d^{Fe}(Ni\text{-}Fe)$. It follows that $n_d^{Fe}<7$ is highly probable for fcc Co-Fe, or that the fcc Co-Fe alloys may correspond to case (c) and exhibit ferrimagnetism.

c. Palladium and platinum. Pd and Pt are Class (2) solvents. As dilute solutes in class (1) solvents, they should carry an induced moment and correspond to ferromagnetic case (d). Data[76] for NiPd and NiPt alloys indicate that, for quenched samples, a linear relationship between $\bar{\mu}$ and c holds up to $c\approx0.4$ for Pd, $c\approx0.2$ for Pt, and that $\Lambda<0.1$ for Ni-Pd, $\Lambda\sim0.6$ for Ni-Pt. The fact that it is difficult to quench order from the Pt alloys renders the latter figure dubious.

If Pd or Pt (or Rh, Ir, Cu, ...) form the solvent, the cases (a)-(d) still apply for the definition of solute-solute interactions. Magnetization measurements have been made on Mn-Pt and Cr-Pt alloys[84,85] that indicate antiferromagnetic nearest-neighbor Mn-Mn and Cr-Cr interactions, ferromagnetic Mn-Pt-Mn and Cr-Pt-Cr interactions typical for case (c). The interactions for Pt-rich Fe-Pt alloys are apparently more complicated.[86,87]

C. Electronic Specific Heat and Hall Effect

The compatibility of the model with the measured γ_{el} for the elements has been built into the constructions of Figs. 6, 7, and 8. Nevertheless, recent measurements[88,61] of γ_{el} for bcc Cr-Fe, Cr-Mn, and Fe-Co alloys appear to provide striking confirmation of the qualitative features of Fig. 6. According to these measurements, γ_{el} approaches a sharp maximum of (40 to 50)$\times10^{-4}$ cal/mole deg^2 at 6.5 electrons/atom. This sharp maximum appears to reflect the lower e_g subband and suggests that this band may be even narrower than shown in Fig. 6. There is also a sharp minimum at

[81] J. S. Kasper and J. S. Kouvel, J. Phys. Chem. Solids **11**, 231 (1959).
[82] P. Weiss, R. Forrer, and F. Birch, Compt. rend. **189**, 789 (1929).
[83] M. Peschard, Compt. rend. **180**, 1836 (1925).
[84] M. Ausworter and A. Kussmann, Ann. physik **7**, 169 (1950).
[85] A. Kussmann and E. Friederich, Z. Physik **36**, 185 (1953).
[86] A. Kussmann and G. V. Rittberg, Z. Metallkunde **42**, 470 (1950).
[87] J. Crangle, J. phys. radium **20**, 435 (1959).
[88] C. T. Wei, C. H. Cheng, and P. A. Beck, Phys. Rev. Letters **2**, 95 (1959).

$\sim$8.35 electrons/atom, and this appears to reflect the boundary at which the upper e_g subband begins to be occupied (see earlier discussion).

Metallic Cr is significant for several of its characteristics. One of these is its Hall constant, which is positive, large and temperature sensitive with an effective hole concentration at 14°C of 0.23 hole/atom.[29] This behavior is without explanation on any previous band-structure model, but it is not at all unreasonable given Fig. 6. The bonding t_{2u} band is three fourths filled and therefore contributes little to the Hall constant. The t_{2g} band is nearly filled, and therefore contributes a large, positive term to the Hall constant since the t_{2g}-electron mobility should be relatively high. Temperature sensitivity follows from the fact that the lower e_g subband is right at the Fermi surface.

A positive Hall constant for V (effective number of holes per atom is 1.09) has also been reported.[29] This again is essentially compatible with Fig. 6 since the t_{2g} band has about one hole per atom and the t_{2u} band is presumed to be about three-fourths filled.

In the close-packed metals and alloys, the shallow s band must dominate the Hall effect to make $R_0<0$. The only known exception to this statement[89] occurs in disordered Ni_3Mn in which the band structure is modified by the formation of Mn-Mn near-neighbor bonding.

D. Number and Form Factors of Outer 3*d* Electrons

Careful x-ray measurements of the atomic scattering factors can be used to determine the number of 3*d* electrons in the transition metals. The technique is to measure the absolute scattering factors and to subtract the "argon core" as calculated by self-consistent techniques for the free atom. Since the radial extension of the 4*s* and 4*p* electrons is such that their scattering factors are negligible at all Bragg angles, subtraction of the "argon core" leaves only the contribution of the outer 3*d* electrons. The original experiments by Weiss and DeMarco[90] claimed to find 9.8$\pm$0.3, 9.7.0$\pm$3, 8.4$\pm$0.3 3*d* electrons associated, respectively, with fcc Cu, Ni, and Co, in good agreement with conventional expectations and those of Fig. 8, but only 2.3$\pm$0.3 and 0.2$\pm$0.4 associated, respectively, with bcc Fe and Cr. This latter result was quite unexpected, and subsequent measurements by Batterman[91] gave approximately six 3*d* electrons for Fe. Komura, Tomiie, and Nathans[92] investigated the number of 3*d* electrons at the Fe_I atoms (all near neighbors Fe_{II}, next-near neighbors Al) of ordered Fe_3Al. Whereas Batterman used a polycrystalline iron sample, Komura, Tomiie, and Nathans used a single crystal. In contrast to Weiss and DeMarco, they studied x-rays in transmission rather than in reflection so as to avoid surface-roughness effects. Finally, the ordered alloy reduced the extinction effects and permitted them to go to smaller Bragg angles. Their experimental results are compatible with $n_d=5\pm1$. The model of this paper calls for $n_d=5$ on bcc Fe, but for a larger radial extension of the three bonding 3*d* electrons which could be responsible for the low number of 3*d* electrons reported by Weiss and DeMarco.

In closing, attention is drawn to the fact that the unpaired *d* electrons in α Fe are apparently spherically distributed.[93,94] This is in contrast to the anisotropic form factors found in Ni and Co.[36] The origin of the anisotropic form factors has already been discussed. A spherical form factor for α Fe is implicit in the model since the electron correlations that stabilize next-nearest neighbors with e_g electrons on one, t_{2g} electrons on the other do not "freeze" these distributions (it is a dynamic effect) and at the same time they introduce, on the average, an equal occupation of e_g and t_{2g} states at any atom.[95] In ordered alloys, on the other hand, the correlations may be frozen in. In fact, this has been shown to be the case for ordered Fe_3Al (see reference 51).

ACKNOWLEDGMENT

I would like to thank Dr. T. A. Kaplan and Professor R. K. Nesbet for several helpful discussions.

[89] R. M. Bozorth, *American Institute of Physics Handbook* (McGraw-Hill Book Company, New York, 1957), pp. 5-237 to 5-239.

[90] R. J. Weiss and J. J. DeMarco, Revs. Modern Phys. **30**, 59 (1958).

[91] B. W. Batterman, Phys. Rev. **115**, 81 (1959).

[92] Y. Komura, Y. Tomiie, and R. Nathans, Phys. Rev. Letters **3**, 268 (1959).

[93] R. Nathans, C. G. Shull, G. Shirane, and A. Andresen, J. Phys. Chem. Solids **10**, 147 (1959).

[94] R. J. Weiss and A. J. Freeman, J. Phys. Chem. Solids **10**, 147 (1959).

[95] Simple extrapolation of Fig. 6 calls for considerably more e_g than unpaired t_{2g} electrons, so that any deviation of the form factor from spherical symmetry should favor e_g electrons.